Accelerated stress testing in proton exchange membrane water electrolysis - critical review.

E. Urbano[b,c,*], E. Pahon[a], N. Yousfi-Steiner[b], M. Guillou[c]

[a] *UTBM, FEMTO-ST, FCLAB, CNRS, Belfort, France*
[b] *Université de Franche-Comté, FEMTO-ST, FCLAB, UTBM, CNRS, Belfort, France*
[c] *Direction Opérationnelle Recherche et Developpement, Michelin Ladoux, Cébazat, France*

Abstract

Proton exchange membrane water electrolysis is a promising technology for the production of green hydrogen because of its ideal coupling with renewable energies. However, the reduction of noble materials and the improvement of efficiency and lifetime are challenges to be overcome in order to make this type of hydrogen cost-effective. This paper proposes an in-depth analysis of the electrolyzer operating conditions: power supply, temperature and water flow rate, associating the degradation phenomena identified at each operating point. A cause-effect map of the electrolyzer degradation allows to identify the stress variables and the operating points of interest according to the failure and the component concerned. A comprehensive literature review of the electrolyzer materials degradation is presented in the first part. Accelerated stress protocols proposed in the literature are also presented under a critical approach. The review of degradation and accelerated protocols thus represents an important conceptual framework for the analysis of stress conditions and the guided design of accelerated protocols, presented in the last part of the paper.

Keywords: PEM water electrolysis, Material degradation, Green hydrogen production, Accelerated testing stressors.

---

[*] Corresponding author

Email address: `edwin.urbano-castano@utbm.fr` (E. Urbano)

Preprint submitted to Journal of Power Sources *September 9, 2024*

Word Count

10616

Abreviations

ALT Accelerated Life Test.

AST Accelerated Stress Test.

BPP Bipolar Plates.

CCM Catalyst-coated Membrane.

DOE Department of Energy.

ECSA Electrochemically Active Surface Area.

EPMA Electron Probe X-Ray Micro-analysis.

EU European Union.

FRR Fluorine Release Rate.

FTIR Fourier-transform Infrared Spectroscopy.

GDL Gas Diffusion Layer.

HER Hydrogen Evolution Reaction.

HFR High-frequency Resistance.

IPCC Intergovernmental Panel on Climate Change.

LSC Long Side Chain.

MEA Membrane-electrode Assembly.

MPL Micro-porous Layers.

NHE Normal Hydrogen Electrode.

NZE Net-zero Emissions Scenario.

OCV Open Circuit Voltage.

OER Oxygen Evolution Reaction.

PEM Proton Exchange Membrane.

PEMFC Proton Exchange Membrane Fuel Cell.

PEMWE Proton Exchange Membrane Water Electrolyzer.

PFSA Perfluorosulfonic Acid.

PTL Porous Transport Layer.

SER Sulfur Emission Rate.

SSC Short Side Chain.

TPB Three-phase Boundaries.

XPS X-ray Photo-electron Spectroscopy.

1. Introduction

The sixth report of Intergovernmental Panel on Climate Change (IPCC) has established five possible scenarios of socio-economic development from 2023 onwards [1]. The scenarios have been established according to greenhouse gas emissions trends forecasts, where fossil fuels have more than 90 % of 2022 total emissions at 36.8 [$GtCO_{2eq}$] [2]. Therefore, there is an urgent need to accelerate the energy transition [3]. Hydrogen has a key role to play in the decarbonization of sectors where emissions are difficult to reduce and alternative solutions do not exist or are difficult to implement, such as heavy industry, shipping, aviation and heavy transport [4]. Hydrogen is therefore gaining acceptance as a substitute to fossil energy and clean energy storage, making its production a key player in the 2050 net-zero emission scenario (NZE) [5, 6].

Among the low temperature electrolysis: alkaline, anion-exchange membrane and proton-exchange membrane, the latter is currently receiving special attention from industry and the scientists [7]. With a maturity comparable to alkaline electrolyzers [8], PEM electrolyzers are gaining importance for two fundamental reasons. The first is their rapid response which makes them suitable for coupling with renewable sources such as solar and wind [9, 10]. The second is the possibility of elevated pressures operation, theoretically up to 85 [bar], and 30 [bar] in the most common applications, thereby reducing the energy for hydrogen compressing [11]. Moreover, the utilisation of Pt group and other noble materials makes the high cost their major disadvantage [12].

The hydrogen economy deployment around the world encourages mass production of PEM devices [13]. The European Union (EU) expects 40 [GW] of electrolyzers capacity by 2030 [14]. Additionally, the regions potential, such as South America, with large capacity for green hydrogen production has been studied by researchers as guidelines for public policies. The green hydrogen production opportunities in South America regions have been explored by Nadateli et al. [15, 16] and specific case like Colombia one has been investigated [17] with the aim of providing a scientific framework for national green hydrogen production plans, being one of the pioneer countries in the region. However, two main points are the main challenges for PEMWE to be commercially competitive: cost and durability [18, 19].

The use of rare materials such as titanium and platinum group metals, like iridium, ruthenium and platinum itself, makes the hydrogen production by PEM an expensive option [20]. To reduce costs, the lifetime becomes a major factor. Markets for electrolyzers claim a lifetime up to $60,000$ [h] or longer [21]. To achieve this objective, two options are the most appropriate. The first and most time-consuming is to change the known electrolyzer designs, including the development of new materials and less costly technologies. The second is the materials and designs optimisation. In short and medium term, the second option is the most suitable. Therefore, a in-depth knowledge of technology degradation is essential [22].

Few reviews on the PEMWE degradation are available in literature. In contrast to fuel cell, the number of reviews is less numerous, but provides important information on the complex phenomena involved in operation. Feng et al. [23] and Khatib et al. [19] present degradation reviews in cell components. Other authors provide reviews with emphasis on improvement potentials: identification of valuable gaps in comprehension and key needs for development [24], latest advances and current challenges towards green and low-cost hydrogen [18] and the most convincing research, from the authors' perspective, on increasing electrolyzer efficiency [25]. A review of test procedures for component and single cell degradation are reported [26]. All the reviews consulted are focused on components materials and single cell.

Test protocols for PEMWE can have several approaches according to the scope: components materials, single cell, stack and system [27]. In-situ and ex-situ tests can be applied in order to evaluate the performance and degradation. The electrolyzer degradation can be observed by durability tests (long duration) and accelerated tests (reduced duration). The urgent need to PEMWE optimisation and reduction of green hydrogen cost makes accelerated testing an urgent need. The scientists are therefore paying attention to accelerated tests development, which have not received the required attention, in contrast to fuel cell [28].

Two different types of accelerated tests are defined by the EU, accelerated stress test (AST) and accelerated life test (ALT) [27]. The main difference is lifetime range covered by each test, while ALT covers the entire lifetime, AST looks for degradation over a portion.

The state-of-the-art on accelerated tests does not provide a clear definition. The accelerated tests proposed under this name are in most cases stressors variations to nominal operation that generate further degradation [26]. However, higher degradation is not a strong argument to set suitable AST, ALT. It must be said that a accelerated protocol is a method that in reduced time enables to achieve comparable results, components degradation, to durability test under equivalent operating conditions. Cost reduction and test time reduction are therefore the main protocol objectives.

Two publications have been reported in the last years under the same axis of the present work, the need for standardised test. First a review of accelerated stress tests by Kuhnert et al. [29]. Second a report by the EU, on the harmonised AST and durability protocols [30]. However, the present work presents an original novelty. Thus, this work goes further by providing the analysis and correlation between electrolysis operating points and degradation phenomena, validated from all the studies included in this work (see graphical summary). The aim of this work is not only to provide the conceptual framework for accelerating degradation, but to do it in a guided and precise way on materials, cells or stacks. This will enable the future design of protocols that allow new developments to be tested and obtain results equivalent to durability tests in reduced times.

This article proposes in the second section a detailed review of the ageing phenomena of electrolysers. In the third section a review of accelerated protocols for components, unit cells and stacks. It ends with the selection and conceptualisation of stressors for AST/ALT under real operating conditions, as well as the operating points that activate the different degradation mechanisms. Thus, the first two parts are a detailed conceptual framework for the analysis presented in the last part of the article. This analysis is motivated by two fundamental reasons. The first is to establish a conceptual framework for the degradation of PEM electrolysers which has been of less interest and with different electrochemical phenomena than their equivalent fuel cell. The second is the development of accelerated ageing protocols that can subsequently become a reference for the standardisation of these tests in order to accelerate the improvement of the technology through the appropriate comparison of results.

2. Components degradation in proton exchange membrane water electrolyzer

A single electrolysis cell of the PEM type is composed of multi-layers assembled at a particular pressure. Polymeric membrane, catalysts, porous transport layers and bipolar plates each perform specific functions with different materials and designs. Fig. 1 provides an overall scheme of an electrolyzer cell, with the main components and reactions. The most common materials used in commercial electrolysers are also introduced.

This section presents the literature review on the degradation phenomena affecting each of cell components. Before degradation phenomena, a thermodynamic principles explanation of water electrolysis is presented to put into context the losses incurred by the ageing processes.

To break down water particles into molecules, an external energy is required. The required energy or the released energy for the chemical bond formation or breaking is estimated as the sum of the products enthalpies of formation, $\Delta H_{f,pdt}$, minus the sum of the reactants enthalpies of formation, $\Delta H_{f,rct}$. The reaction total energy required is then known as the reaction enthalpy, ΔH_R. The water splitting process is boosted by an electrical and thermal input energy [31]. ΔH_R can be written as the sum of these factors.

$$\Delta H_R = \Delta G_R + T \cdot \Delta S_R \tag{1}$$

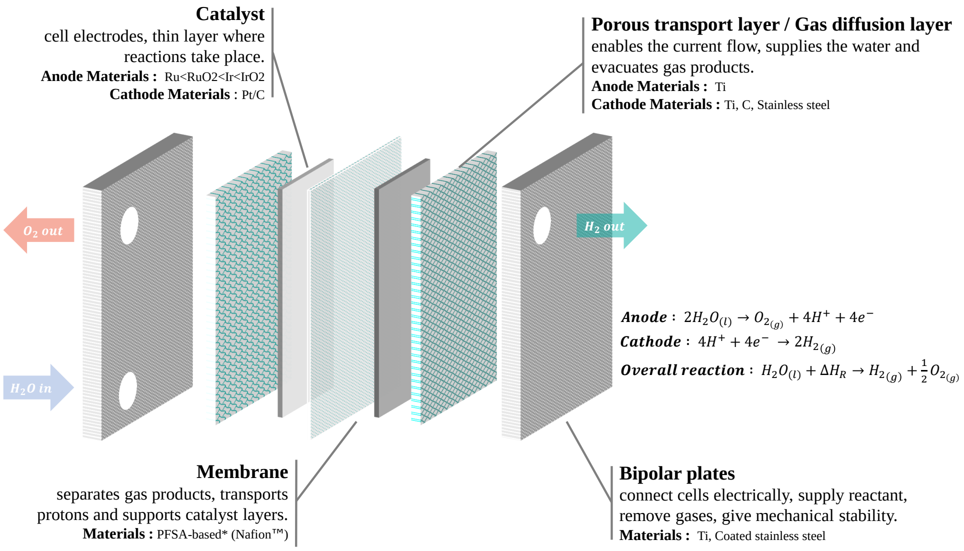

Fig. 1: Sketch of a proton exchange membrane electrolysis cell

The term, ΔG_R, is the Gibbs free energy transition. This thermodynamic quantity represents the maximum work that can be extracted from the thermodynamic system, without the volume work. $T \cdot \Delta S_R$, the entropy multiplied by the system temperature T, is known as the entropy factor and stands for the chemical reaction heat input. At standard state (25 $[°C]$ and 1 $[atm]$), ΔG_R^0 is $236.483[kJ \cdot mol^{-1}]$ and ΔH_R^0 is $285.83[kJ \cdot mol^{-1}]$ [32]. Taking Faraday constant, F, and the number of charges, z, transferred in reaction, V_{rev}^0, in a reaction with an external heat source, can be calculated by following equation.

$$V_{rev}^0 = \frac{\Delta G_R^0}{z \cdot F} = 1.229\ [V] \tag{2}$$

For a reaction without an external heat source, V_{th}^0, can be calculated as follow.

$$V_{th}^0 = \frac{\Delta H_R^0}{z \cdot F} = 1.481\ [V] \tag{3}$$

The voltage calculated with or without external heat input for an electrolysis cell are known as the Open Circuit Voltage (OCV) at lowest heat value and highest heat value, respectively. However, as the current flows through the cell, voltage is considerably higher because of non-reversible internal cell losses. It exists three main kinetic losses sources in a PEMWE cell: anodic and cathodic activation, ohmic, and mass transfer losses [33].

The losses can be group as faradaic and non-faradaic. As faradaic losses are the activation losses, which are generated due to the transfer of electrons between the redox couples at the electrode/electrolyte interface of Oxygen Evolution Reaction (OER) and Hydrogen Evolution Reaction (HER). This process results in irreversible losses called activation over-potentials present at both the anode and cathode electrodes [34]. Cathodic and anodic activation losses are commonly analysed separately in order to identify the contribution of each. Anodic losses are predominantly due to the harsh electrochemical environment.

The losses generated by non-faradaic mechanisms are ohmic and mass transport losses. The best known, ohmic losses are due to the electrons flow resistance through the electrodes and cell components and the proton resistance in membrane. These losses behave according to Ohm's law, so they are directly proportional to the amount of current flowing through the cell. Finally, mass transport losses are due to diffusion and bubble over-potentials. Both mechanisms are evident at high current densities when gas production is important. Diffusion losses happen when the gas bubbles block part of current collectors pore network, while bubble overpotential arises when very large gas bubbles shield the Electrochemically Active Surface Area (ECSA), reducing the catalyst utilisation and hindering the reaction [35].

The real electrolysis voltage in the cell is then the sum of the OCV, plus all the internal cell losses. The Nernst equation for OCV, the Butler-Volmer equation describing the activation losses, Ohm's law for the ohmic losses and the modelling equations for diffusion losses can be consulted by the reader at [5, 36, 37]. Fig. 2 shows a theorical polarisation curve with kinetic losses contribution calculated from the equations presented in the given references.

Finally, it is relevant to specify that degradation is understood as the loss of electrolyzer performance [27], which means a cell voltage increase, represented by previous losses explained, therefore a greater energy consumption.

2.1. Electro-catalyst layers

These thin layers of about 10 μm are where the reaction takes place thanks to the Three-phase Boundaries (TPB). At the anode they allow the formation of O_2 and H^+ on contact with the water molecule, while on the cathode side the hydrogen protons recover the electron they lack to form

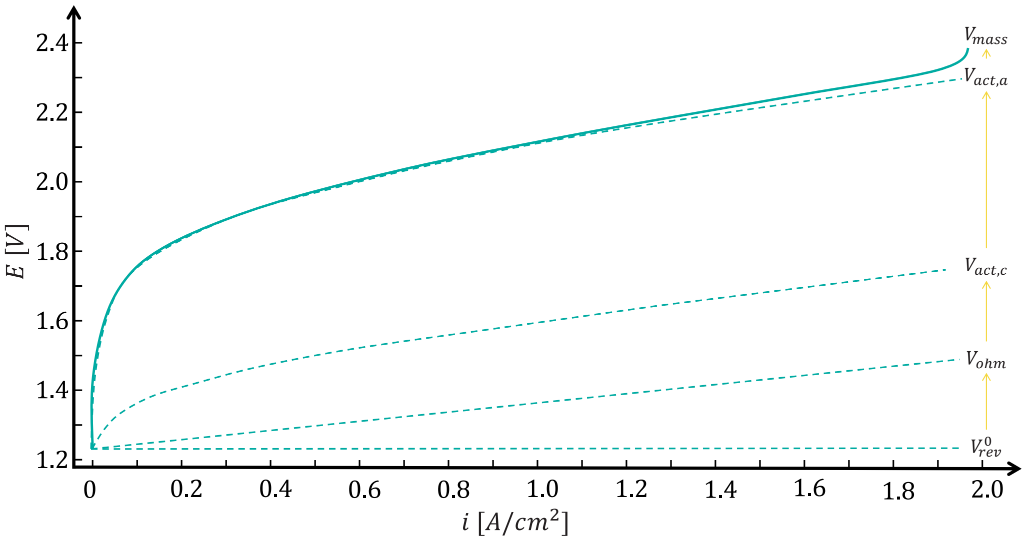

Fig. 2: Theorical polarisation curve for PEMWE, with losses contribution

H_2. At both the anode and the cathode, these electrodes are generally of a support and a metal designed to maximise the contact surface and the efficiency of the reaction.

Its fundamental function makes the viability of hydrogen production by water electrolysis dependent on the long-term supply of abundant and durable electrocatalyst materials and the overall efficiency of the process [38]. In addition, the harsh electrochemical environment, with high voltages and high oxygen concentrations, limits the choice of materials to noble metals: Pt (platinum) groups [23]. At anode, for the oxygen evolution reaction (OER), investigations into the activity-stability relation have concluded that the most active oxides in platinum group metals show the lowest stability [39]. The researchers have obtained the following results: $Au \ll Pt < Ir < Ru \ll Os$ for activity and $Au \gg Pt > Ir > Ru \gg Os$ for stability. Thus, the most adopted materials for OER are Ir (iridium) and Ru (ruthenium) based [40, 41], with Ir based catalysts, specially IrO_2, being the most viable option because of its high level of activity and stability [42]. Since the utilisation of Ir strongly impacts the production cost of PEMWE the most direct way to save costs would then be to use Ir-free catalysts, but it is also the most difficult. Studies on catalysts from non-noble materials are fairly rare in the literature. Consequently, the main objectives in research on catalyst are to decrease the amount of precious metals as catalysts and to increase their stability. Currently, the Ir loading in commercial electrolyzers is $2-2.5$ $[mgr \cdot cm^{-2}]$, but it is estimated that a loading of $0.05-0.1$ $[mgr \cdot cm^{-2}]$ could reach the gigawatt scale [43]. However, direct load reduction will result in an irreversible loss of performance [44].

Although the hydrogen evolution reaction (HER) is not the critical point (proton reduction is about 100 million times faster than OER) [11, 45], few known metals have such high activity and long-term stability as Pt. These characteristics make platinum the reference catalyst for HER [46]. Recent research shows promising results with new materials for HER. Ramakrishna et al. [47] use nitrogen-doped carbon nano-tubes supported by palladium electrocatalysts as hydrogen electrodes and Jeong et al. [48] present a method for the production of transition metal carbide nanocrystals as a promising substitute for the Pt/C catalyst. Some authors also present reviews on noble metal-free electrocatalysts as a viable option for electrolysis [49, 50]. Currently commercially available electrolysers mostly use platinum-based catalysts, so that large-scale production of PEMWE is limited by the expensive and rare platinum catalyst. It is to be expected that this will evolve in the years to come thanks to the great efforts of the scientific community to develop more durable materials.

Catalysts degradation has been observed at both the cathode and the anode and electrochemical phenomena affect the catalysts themselves as well as the support, especially titanium used as support at anode [51]. Due to the harsh conditions multiple phenomena can degrade the catalytic layers, affecting their durability and stability. From the literature, catalyst dissolution, agglomeration and migration, contamination by external ions, passivation and corrosion of support were acknowledged as mainly responsible for the performance drop of the catalyst [23]. Researchers have found that these phenomena also affect the degradation of other components such as the gas diffusion layer and the membrane [29]. The degradation of the catalyst is evidenced by changes at catalyst/membrane interface due to the thinning of the catalytic layer. Consequently, the ECSA is reduced (rise of the activation voltage), which leads to a rise in the electrical contact resistance.

2.1.1. Catalyst dissolution

Since iridium oxide is the most viable OER material [41, 43] and the anode is the most affected by catalyst dissolution due to the high voltages it is subjected to (> 1.5 [V]), researchers have focused on studying its dissolution. This phenomenon leads to a progressive loss of electrolysis performance due to the catalytic thinning resulting in an increase of the kinetic losses during extended operation [52]. Therefore, the study of this phenomenon is crucial to improve the performance, even if it is not a source of abrupt cell failures. There is a wide agreement among scientists on the circumstances of the Ir dissolution. Ir dissolution process proposed by Cherevko et al. [53, 54] is referenced. They have concluded that the formation of iridium complexes, like $Ir(OH)_3$ and Ir_2O_3, is the main cause for this phenomenon. These complexes are renowned for their unstable nature and high relative water solubility near low pH. Cherevko et al. [53, 54] provide more details on the iridium complex formation.

From the conducted studies on iridium dissolution and the durability and stability of these nanoparticles, the researchers have concluded that the mass activity and electrochemically active surface are (ECSA) degrade most seriously at high cell voltage (> 1.8 [V]). They also state that mass activity losses begin at medium voltage ($1.4-1.6$ [V]) [55]. However, the efficiency and catalyst activity improve at high voltage ranges [56]. Shirvanian et al. [57] suggest three different pathways of Ir dissolution depending on the operating voltage and the catalyst surface structure: (i) direct metal Ir dissolution at lower voltages, close to open-circuit voltage in iV curve (see Fig. 2), (ii) IrO_3 generation at high voltages, and (iii) transition from the $Ir_V - Ir_{III}$ oxidation state at intermediate voltages. To detect those phenomena in the catalytic layer due to the detachment of particles diffusing into the porous transport layer (PTL), some researchers propose for example in-situ methods [58].

Although studies on the dissolution of platinum are less frequent, there are some findings in the literature. Dodwell et al. [59] show for open circuit voltage (OCV) periods that at a cathodic potential higher than 0.85 [V] against the normal hydrogen electrode (NHE) platinum dissolves because of oxygen scattering from the anode side. At the greatest cathodic voltage of 1.02 [V] against NHE, the dissolution rate reached its maximum. Experimental evidence presented by the researchers shows that in periods of OCV the platinum from the cathode and the oxides formed migrate towards the membrane causing a loss of active surface area or dissolve in the outflow water. The same phenomenon can potentially be detected on the anode side when Pt is used as a catalyst for OER [60]. It would therefore be relevant to highlight that the platinum deterioration has a role to play that is more important than is generally realised [61].

2.1.2. Support passivation

As a consequence of the oxygen presence, the build-up of a non-conducting oxide coating on the anodic catalyst reduces the electron flow and increases the contact resistance (higher cell voltage) [62]. The passivation of Ti (titanium), used as a support for iridium oxide, seems to be more important at high current densities [63] and/or in the presence of pollutants such as fluoride (dissolved from the membrane) or contaminants in the water flow such as iron ions, Fe^{x+} [23].

2.1.3. Particles agglomeration and migration in the catalyst

Nano-particles are basically unstable at the atomic scale due to their growth caused by agglomeration and migration. Catalyst agglomeration is then defined as the rise in particle size because of sintering or crystal growth throughout time [64]. The causes of this phenomenon have been investigated for the fuel cell, but this is not the case for electrolysis, however this phenomenon has also been evidenced in PEMWE [65]. From the investigations conducted on fuel cells, several mechanisms, which can occur separately or together, have been proposed as the source of this phenomenon: (i) coalescence via crystal migration, (ii) growth via modified Ostwald ripening, and (iii) re-precipitation at other nucleation sites [62, 66]. The agglomeration of the catalyst then leads to a significant ECSA loss, resulting in cell efficiency decrease. Research has also shown that this phenomenon leads to a decrease of the exchange current density at the cathode side.

Catalyst agglomeration and migration has been reported in the cathode and the anode. This process is accelerated under harsh operating conditions, particularly the applied voltage [67]. For the anode catalyst some researchers have reported that operating voltage affects ionomer degradation. The latter is the main known cause for the agglomeration of iridium oxide [68, 69]. Paciok et al. [70] reveal through analysis of X-ray photo-electron spectroscopy (XPS) that at a lower overpotential (i.e., the voltage difference between V_{th} and the potential at which the redox event is observed, E_{cell}.), the rate of hydrogen coverage of the Pt particles is enhanced, resulting in a wider gap between the carbon support and the Pt particles. Thus, the increased mobility of the Pt particles due to the weakening of the Van der Waals forces promote the catalyst agglomeration [70].

2.1.4. Metallic cations poisoning

Ionic cationic pollutants come from the feed water, from corrosion of the system and stack metal parts, and from the membrane-electrode assembly (MEA) manufacturing [71]. These contaminants occupy the ion exchange sites between the polymer membrane and the catalytic layer, resulting in an enhanced charge transfer resistance and, consequently, an increased voltage at both the anode and the cathode. The inherent reactivity of the catalyst, especially the Pt, is also affected because external contaminants can occupy the catalyst interface (i.e., the surface active spots) [72].

Contaminants from other cell components, such as Ti, have also been evidenced in the cathode catalyst [73]. Titanium particles that are corroded during operation migrate to the cathode catalyst resulting in a reduction of the proton mobility in the ionomer and a reduced cathodic exchange current density. This phenomenon has been evidenced in the anodic catalyst as well. However, it has been reported in the literature that the contamination by metal cations is mainly a reversible process. The contaminates can be removed by immersing the MEA in liquid acid solution (i. e., H_2SO_4 solution) [74, 75].

2.2. Polymer membrane

This polymer electrolyte used in PEM technology can range from 100 to 200 μm. Its main function is the conduction towards the cathode of the H^+ protons formed in the anode, as well as the separation between the products and the reactants, thus ensuring safety. The electrolyte with the anode and cathode electrodes is called the MEA (see Fig. 1).

As for PEMFC, the membrane is a crucial component for electrolyzers, as it determines the transport phenomenon, the performance, and the durability of the technology [76]. However, in terms of efficiency, reliability, durability and security, the membrane is the cell's weakest element [77]. The presence of materials like hydrogen and oxygen on each membrane side also makes this component vital for safe operation and to avoid sudden failures. This makes the lifetime of the technology conditional on the durability and stability of the polymer layer, making the development of durable MEA for electrolyzers one of the main challenges in the technology improvement. Understanding degradation phenomena is the main need for the development of more economical, efficient, and durable MEA [64].

The PEM, based on polystyrene sulphonic acid, was applied for the first time in the 1960s for the Gemini spacecraft. At the beginning of the

1970s, Dupont further developed the perfluorosulfonic acid (PFSA)-based Nafion®series membranes, which provide higher proton stability and conductivity [76]. At present, there is a wide variety of proton exchange membranes and new technologies are being proposed [78], with novel and appropriate assembly methods [79, 80]. Today the PFSA membrane is still considered the most popular. Depending on the side chain length and the CF_3 content, the membrane can be classified as long side chain (LSC) [81, 82] and short side chain (SSC) [83, 84], represented by Nafion® from DuPont and Aquivion® from Solvay Solexis, respectively. Based on the analysis of its chemical composition, the LSC PFSA membrane has a better mechanical stability and better proton conductivity, and other favourable features, making Nafion®the most widely accepted membrane [76].

In contrast to fuel cell, where many research studies have been conducted to determine degradation phenomena affecting the membrane [81, 85–88], few studies are available on PEMWE [89, 90]. Even though PEMFC is the inverse process of PEMWE, the degradation phenomena are not similar in most cases due to the different hydration state, different operating conditions, and dissimilar mechanical forces on the membrane. The intermediate reactants created in the electrolysis dissolve efficiently without the risk of under-saturation of the reactants, as it is known for the fuel cell [91]. This is because the electrolyzer membrane is completely immersed in water, which also prevents stress due to hydration and dehydration. However, complete submersion of the membrane can cause it to swell with a consequent decrease in its mechanical strength and integrity [92]. In addition, electrolysis membranes exhibit less chemical degradation than fuel cell membranes. According to Feng et al. [23] the degradation phenomena affecting the membrane can be classified as chemical, thermal and mechanical.

2.2.1. Chemical membrane degradation

Membrane chemical degradation is due to two main sources: (*i*) thinning of the membrane due to ionomer degradation which is attacked by radicals, like hydrogen peroxide (H_2O_2) and related species such as hydroperoxyl ($HOO^\bullet$) and hydroxyl ($HO\bullet$), formed due to gas crossover [93] and (*ii*) contamination by external metal ions from the feed water or other cell metal components (i.e., titanium oxides and Fe^{x+}) [77]. The first phenomenon generates a permanent loss of performance and can be evidenced by mensuration of the fluorine release rate (FRR), in addition to the sulphur emission rate (SER) in the output water at the cathode and the anode. The second phenomenon is reversible by treating the MEA in an acidic solution, as sulphuric acid solution [94].

Degradation due to radical attack is commonly observed with membrane thinning measured by post-mortem analysis [95] or FRR and SER rates with in-situ measurements [96]. The fluorine and sulphur release that causes membrane thinning is generated by the degradation of the perfluorosulphonic acid backbone attacked by oxidative species. From literature the oxidative level of principal radicals involved in ionomer degradation for polymer membranes can be classified as follows: $HO^{\bullet} > H^{\bullet} > HOO^{\bullet} > H_2O_2$ [97]. Chain scission, release and loss of functional groups are caused by attack on the ionomer by these oxidising species. Table 1 shows the principal reactions that involve the radical's formation in membrane with the corresponding formation kinetics coefficients. Some researchers conclude that the reaction involving degradant radicals are catalysed thanks to gases crossover from the cathode to the anode side [98], measured by special sensors or in-situ methods [99]. Gas crossover is enhanced at the same time by the membrane degradation, notably the thinning due to the fluorine dissolution, then an effect-cause cycle and reverse can occur. From what is known in the literature about mass transport in PFSA-based membranes there are still mechanisms to be clarified [35] and the transport of water, protons and gas crossover are believed to be impacted by operating conditions such as pressure, temperature and current density [100]. Chandesris et al. [90] have developed a model describing the membrane chemical degradation based on the radical-involved chemical reactions proposed by Gubler et al. [97]. In their research they have concluded that temperature and low current intensities ($> 80°C$ and i near to OCV) strongly impact polymer degradation.

Among the metal ions coming from the feed water such as Ca^+, Cu^+, Fe^{x+}, or titanium ions due to oxidation of other cell parts, the most membrane-degrading would be iron ions. Wang et al. [71] have shown in their experiments that for the Nafion®, Fe^{x+} have a higher attraction to sulphonic sites than H^+. This causes an increase of the activation loss, reduction of the proton concentration and conductivity due to the decrease of the effective area of the three-phase boundaries (TPB). With electron probe X-ray micro-analysis (EPMA) Sun et al. [75] further illustrate for a stack with 7.800 $[h]$ operation that the elements Ca^+, Cu^+ and Fe^{x+} are distributed in the membrane and catalyst of catalyst-coated membrane (CCM). The loss of stack performance, as evidenced by different characterisation techniques, was mostly caused by metal cations poisoning.

#	Reaction	Proposed rate
1	$HO^\bullet + R_fCF_2COOH \longrightarrow products$	$< 10^6 M^{-1}s^{-1}$
2	$HO^\bullet + PSSA \longrightarrow products$	$4x10^8 M^{-1}s^{-1}$
3	$H_2O_2 \longrightarrow 2HO^\bullet$	$1.2x10^{-7} s^{-1}$
4	$HO^\bullet + H_2O_2 \longrightarrow HOO^\bullet + H_2O$	$2.7X10^7 M^{-1}s^{-1}$
5	$HOO^\bullet + H_2O_2 \longrightarrow HO^\bullet + H_2O + O_2$	$1M^{-1}s^{-1}$
6	$HO^\bullet + H_2 \longrightarrow H^\bullet + H_2O$	$4.3x10^7 M^{-1}s^{-1}$
7	$H^\bullet + O_2 \longrightarrow HOO^\bullet$	$1.2x10^{10} M^{-1}s^{-1}$
8	$2HOO^\bullet \longrightarrow H_2O_2 + O_2$	$8.6X10^5 M^{-1}s^{-1}$
9	$Fe^{2+} + H_2O_2 + H^+ \longrightarrow Fe^{3+} + HO^\bullet + H_2O$	$63M^{-1}s^{-1}$
10	$Fe^{2+} + HO^\bullet + H^+ \longrightarrow Fe^{3+} + H_2O$	$2.3X10^8 M^{-1}s^{-1}$
11	$Fe^{2+} + HOO^\bullet + H^+ \longrightarrow Fe^{3+} + H_2O_2$	$1.2X10^6 M^{-1}s^{-1}$
12	$Fe^{3+} + HOO^\bullet \longrightarrow Fe^{2+} + H^+ + O_2$	$2X10^4 M^{-1}s^{-1}$
13	$Fe^{3+} + H_2O_2 \longrightarrow Fe^{2+} + H^+ + HOO^\bullet$	$4X10^{-5} M^{-1}s^{-1}$

Table 1: Summary of reactions involving the formation of radicals degrading the polymeric membrane [97]

2.2.2. Thermal membrane degradation

High efficiency in electrolysis is clearly one of the main axes of technology optimisation for obtaining low-cost green hydrogen [101]. High temperatures ($80-100$ [$°C$]) could clearly improve the capacity of membrane for ion transport and enhance the electrochemical reaction rate [76]. However, it is known from the literature that excessively elevated temperatures (> 80 [$°C$]) can reduce the quantity of water and degrade the material leading to membrane failures. Some studies have shown that temperature is higher stress factor than current intensity [94]. Thermal degradation of Nafion® like chemical degradation, begins with by the decay of the lateral acid sulphonate group, as shown in Fig. 3 [102]. Membrane thermal degradation in automotive fuel cell applications is reviewed by Zhao et al. [103] and Chandesris et al. [90] provide a model and experimental evidence of the large impact of temperature on membrane thinning. Their work shows evidence of the important effect of operating temperature on the dissolution of the functional groups on the polymeric membrane, which is strongly accelerated at temperatures above 80 [$°C$].

Cold start processes are also degrading for the membrane. For fuel cells, it shows by Alink et al. [85] that the water contained in the membrane, which is mainly contained in the polymer chains, is evacuated making it

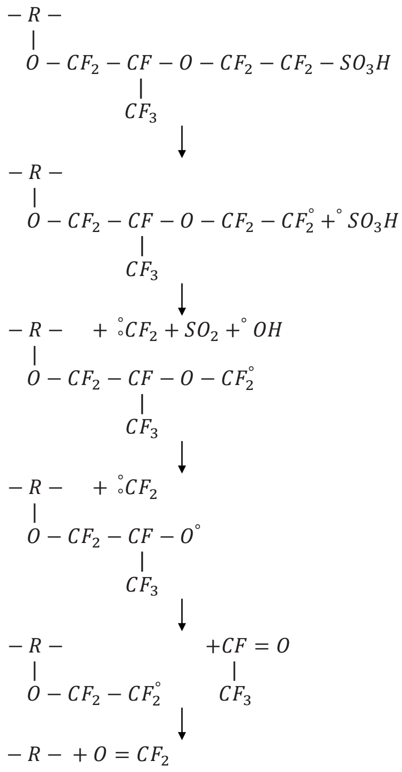

$$\begin{array}{l} -R- \\ \ | \\ O-CF_2-\underset{\displaystyle CF_3}{\underset{|}{CF}}-O-CF_2-CF_2-SO_3H \end{array} \qquad (1)$$

$$\downarrow$$

$$\begin{array}{l} -R- \\ \ | \\ O-CF_2-\underset{\displaystyle CF_3}{\underset{|}{CF}}-O-CF_2-CF_2^{\circ}+{}^{\circ}SO_3H \end{array} \qquad (2)$$

$$\downarrow$$

$$\begin{array}{l} -R- \quad + {}^{\circ}_{\circ}CF_2+SO_2+{}^{\circ}OH \\ \ | \\ O-CF_2-\underset{\displaystyle CF_3}{\underset{|}{CF}}-O-CF_2^{\circ} \end{array} \qquad (3)$$

$$\downarrow$$

$$\begin{array}{l} -R- \quad + {}^{\circ}_{\circ}CF_2 \\ \ | \\ O-CF_2-\underset{\displaystyle CF_3}{\underset{|}{CF}}-O^{\circ} \end{array} \qquad (4)$$

$$\downarrow$$

$$\begin{array}{l} -R- \\ \ | \\ O-CF_2-CF_2^{\circ} \end{array} \quad +\underset{\displaystyle CF_3}{\underset{|}{CF}}=O \qquad (5)$$

$$\downarrow$$

$$-R-\ +O=CF_2 \qquad (6)$$

Where, $-R-$ *is the polymer backbone:* $-(-CF_2-CF_2-)_m-(-CF-CF_2-)_n-$

Fig. 3: Schematic diagram of the loss of the side chain in a polymeric membrane of the LSC type [102]

more likely to freeze on the membrane surface. No freezing of the polymer chains will occur until the water saturation in the membrane [85]. Thus, the membrane surface is affected by the swelling volume of ice expansions that can form pinholes and cracks. This phenomenon can even delaminate the catalyst [104].

2.2.3. Mechanical membrane degradation

Mechanical degradation are considered more probable than thermal and chemical degradation and can cause sudden and premature failures of the electrolyzer [77]. Membrane stress can be related to different factors of cell and/or stack operation, as well as the clamping force on the stack assembly. For fuel cells, Khorasany et al. [88] found a close link between membrane stress and operating conditions, such as voltage, temperature and relative humidity. In contrast to fuel cells for electrolyzers, mechanical failures caused by membrane drying are less likely due to total submersion in water but swelling phenomena can be more probable.

Mechanical failures can manifest as cracks, tears, pressure of reagents and stress [104]. Excessive clamping force can lead to cracking in the contact zones with the bipolar plate channels and non-uniform compression between the porous transport layers can also ruin the membrane [105]. Membrane pinholes represent a safety issue due to potential hydrogen and oxygen combustion. Mechanical failures can also be due to a non-optimal water flow rate. When the water flow rate is too high, a pressure accumulation takes place, which can destroy the membrane electrode assembly [106]. On the other hand, insufficient water flow affects the electrolysis performance and leads to an unequal distribution of the water through the channels of the bipolar plate, resulting in an unequal distribution of the electric current [107]. An in-homogeneous current distribution can lead to membrane swelling and the formation of hot spots that increase the degradation rate as it is an exothermic reaction at high voltage [108].

2.3. Gas diffusion and porous transport layers

These porous layers, external to the catalytic layers (see Fig. 1), have as their main function bi-phase mass transport (reactant delivery and product removal), electrical conduction and mechanical support. Their designs generally consist of nano to naked-eye visible fibres arranged to form a porous layer. The materials used may differ between cathode and anode and some may be coated with noble metals to prevent oxidation.

The designation of these layers is varied in the literature. Some authors refer to it as current collectors and others make distinctions between anode and cathode, naming gas diffusion layer (GDL) for the cathode, as it is called in fuel cell, and porous transport layer (PTL) for the anode [29]. In order to differentiate between the anode and cathode side, in this work, GDL will be used as the term for the cathode and PTL for the anode.

In contrast to PEMFC, the materials choice is limited for electrolysers. The high voltages and high oxygen concentration in the anode part mean that carbon (a material commonly used in fuel cells) can only be used in the cathode part, where hydrogen is produced [109]. The choice of materials for electrolysis is then reduced to Ti and stainless steel. Although the function of supplying the reactants to the MEA and evacuating the products is vital to the operation of the electrolyzer, contrary to catalytic layers and polymeric membrane, the number of studies available on GDL/PTL are limited. From those studies it is known that the main degradation phenomena are due to materials corrosion. Degradation GDL/PTL for can be classified as chemical and mechanical [23].

2.3.1. Chemical degradation

The chemical degradation of GDL/PTL clearly depends on the material used and operation environment (i.e., O_2 presence and voltage). Cathode-side GDL, unlike PTL, suffer less from corrosion due to insufficient cathode voltage (approximately 0.1 $[V]$) and non-rich oxygen environment [110]. On the other hand, the titanium used for PTL has a more important chemical degradation due to high voltage and rich oxygen environment. Although titanium is the most corrosion resistant material in acidic and high voltage environments, phenomena such as hydrogen embrittlement, passivation and corrosion are well evidenced in the operation of electrolysis cells [111].

Knowledge of degradation in GDL/PTL is a crucial issue for optimising hydrogen production, as improving its efficiency can enhance the overall efficiency of the electrolyzer, better transport of mass and electrons are able to provide a proper environment for the MEA. To achieve an optimal GDL/PTL design, some challenges have to be overcome, such as pore size and shape, layer thickness and more durable and corrosion resistant materials, especially on the anode. Thus, titanium-based PTL is highly passivated in anode conditions and a non-conductive layer is formed at the surface [112]. The oxides formed at GDL can dissolve and contaminate the membrane reducing the ECSA. The different forms of titanium can be coated with platinum group metals or gold to avoid such degradation. However, the application of coatings further increases the already high cost of these components [113]. In response to the high cost of titanium PTL, stainless steel appears to be a viable option, still with corrosion phenomena affecting these components [114]. Hydrogen embrittlement is another phenomenon that affects Ti components degrading layers, which can lead to dissolution of the material in the water outlet and loss of contact between the adjoining components. Lu et al. [115] have performed a study of the resistance of materials to hydrogen embrittlement and concluded the following: $Ti = Ta > Nb > Nb > Zr > graphite$. Therefore, titanium is the most resistant material to this phenomenon while graphite is the most susceptible. The understanding of PTL degradation phenomena allows the development of optimal structures, where interaction with catalyst layer is a critical issue. Some authors for example propose the methods for direct deposition of anodic catalyst in PTL in order to avoid loss of contact during operation and improve electrolysis efficiency [116].

At GDL conditions are less degrading. Carbon-based material can be used reducing the price and building on the knowledge already available on PEMFC. Even if carbon-based GDL are less affected than PTL, corrosion has been reported at cathode side as well affecting overall performance [117].

2.3.2. Mechanical degradation

High compression between the different cell layers is required to avoid water and gas leakage and to arrange minimal contact resistance. However, the compression force greatly influences the properties of the GDL/PTL, as well as the interface with the neighbouring layers (i.e., catalyst and bipolar plates) [5]. Higher compression pressure improves the contact between fibres and other components and improves thermal and electrical conductivity. On the other hand, a high compression pressure leads to noticeable breakage or even displacement of the carbon fibres, which changes the overall morphology of the structure and affects the current transport and fluid permeability [109]. The cell clamping pressure is a main contributor to the proper functioning of the cells. An in-homogeneous pressure distribution in the electrolysis area can cause excessive current maldistribution, due to the overriding of in-homogeneous electrical contacts, causing local degradation in the GDL/PTL and the MEA [118]. Special attention to clamping pressure at assembly procedure is vital to avoid mechanical damage.

For fuel cell applications, Lee et al. [119] have explored the influence of temperature on the durability of gas diffusion layer applying compression strain under steady-state and freezing conditions. Research have found at high temperature (120 [$^{\circ}C$]) a maximum strain of 2.0 % and no influence of freezing was reported for GDL.

2.4. Bipolar Plates

As multi functional components, bipolar plates are in charge of reactants delivery and products removal, as well as providing mechanical support and electrically connecting the cells [23]. In addition to excellent electrical conductivity, the material used for bipolar plates requires high corrosion resistance and low gas permeability [110]. Few materials have an adequate level of these characteristics. Previous studies have been developed in order to assess the viability of several materials, with titanium being the most used. The use of titanium for the manufacture of bipolar plates then represents 48 % of the total cost of an electrolysis cell [114].

It is possible to use more cost-effective materials, such as stainless steel, but this type of steel must be protected against corrosion, especially in the harsh anodic conditions. Some researchers, such as Gago et al. [114], present research on the use of stainless steel in electrolysis processes with promising results. The researchers have concluded that although the corrosion of stainless steel is more significant compared to that of titanium, understanding this phenomenon in electrolysis could be of great help in improving the overall efficiency [120].

In addition to corrosion, another phenomenon affects both titanium and stainless steel, hydrogen embrittlement. The most effective solution is protection with noble metals, further increasing its cost [121]. However, novel research such as that of Liu et al. [122] proposes hybrid coating solutions that use conductive polymers for $Ti - BP$ protection. More research is still needed to achieve a compromise between cost and efficiency in order to improve production costs [123].

Available studies on the degradation of titanium/stainless steel components provide important information, but less numerous than for membrane and catalysts. However, some of the studies carried out for fuel cells can be very useful if the operating conditions are similar (better equivalence for the cathode). Hydrogen embrittlement and passivation are presented in this section as principal degradation phenomena for bipolar plates.

2.4.1. Hydrogen embrittlement

Even if titanium and stainless steel have excellent corrosion resistance and high mechanical flexibility compared to graphite, hydrogen embrittlement is one of the main degradation factors. This implies that hydrides (i.e., TiH_2) can develop on the face of the plates leading to material weakness and possible cracking under stress [5], the formation of non-conductive layers hinders the proper transport of electrons and increases the contact resistance. Lettenmeier et al. [64] have reported that the cathodic part is mostly affected by this phenomenon and also a strong influence of temperature on the formation of hydrides, particularly important when temperatures exceed 80 $[^\circ C]$. High voltages are also a driver for TiH_2 formation. Noble metal protection is often used to prevent premature degradation of bipolar plates and their operation at higher voltages. However, such techniques considerably increase the cost of electrolysis cells [114].

2.4.2. Metal passivation

The conditions under which electrolyzers are operated lead to the passivation of metal components, titanium or stainless steel based. According to the Pourbaix diagram, Fig. 4, titanium is certainly passivated at important voltage, humid and rich-oxidized conditions, such environment can easily be found at anode side in PEMWE. The oxide coating created on the face of the material is not electrically conductive and increases the contact resistance [124]. Platinum group metals and noble metal coatings are generally used to improve the corrosion resistance and to avoid premature erosion. However, the use of such procedures greatly increases the cost of the bipolar plates. Therefore research into novel coatings has been carried out for electrolyzer and fuel cell [125, 126].

For stainless steel, researchers have found that high positive potentials at the anode can promote the formation of oxides [120]. The researchers present evidence that, at high applied potentials, corrosive iron and nickel elements are transferred from the anode to the cathode across the membrane. MEA performance is affected by oxide contaminants that occupy the TPB and reduce the ECSA. These particles contaminate the catalysts and polymer layers, increasing their resistance.

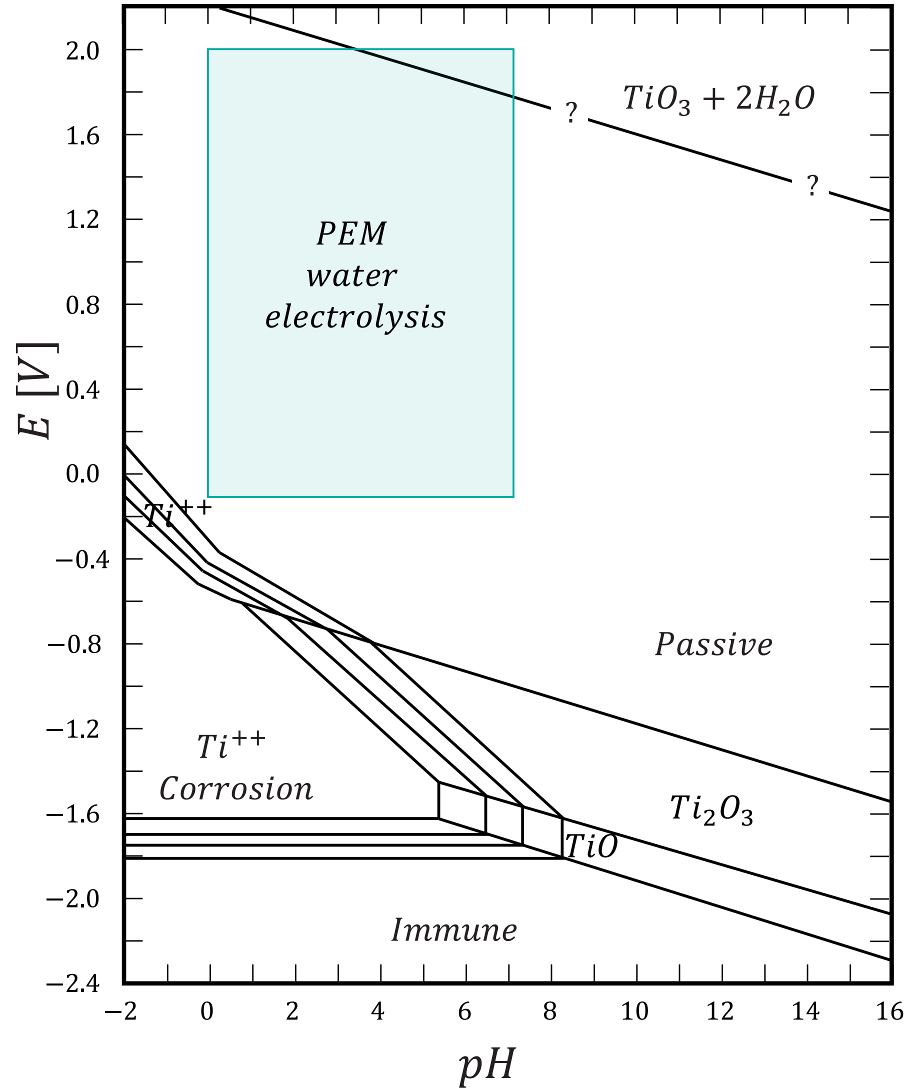

Fig. 4: Pourbaix diagram of the titanium–water system (Potential, pH) [5]

3. Accelerated stress test for proton exchange membrane water electrolysis

Accelerated protocols have been poorly explored for electrolysis, while for fuel cell there are a considerable number of studies proposing such protocols [127]. Available studies appear to differ in their understanding these protocols [26]. Furthermore, most of the protocols proposed for accelerated degradation are not comparable with each other since the test conditions are not defined and and the report on harmonised protocols proposed by the EU is still recent [30], so the results should appear in the next few years. The durability of PEMWE is explored through durability tests which consist of monitoring the voltage variation until the cells end of life. Durability testing represent long periods with significant costs. Currently electrolyzers are able to have a duration up to $20,000$ $[h]$, their degradation has an average up to 14 $[\mu V \cdot h^{-1}]$ [128]. Then, the development of accelerated protocols (AST, ALT) is therefore needed for the technology enhancement and market competitiveness.

In the introduction of this paper, it has been proposed a definition of accelerated protocols: "Accelerated protocol (AST, ALT) is a method that in reduced time enables to achieve results (components degradation) comparable to durability tests, thanks to the application of methodologies that make it possible to establish test conditions based on real operating conditions." For fuel cells, there is a clear definition of AST proposed at European level [129] and some authors propose methodologies in line with this definition. Escribano et al. [130] for example propose a two-step methodology: (i) The degradation phenomena induced by ageing tests following a load profile and operating conditions typical of real cycles are taken as the starting point, (ii) subsequently, modified load cycles were defined to exacerbate the degradation and induced voltage losses, maintaining the same mechanisms involved and allowing a similar level of performance to be achieved after a shorter test period. A comprehensive review for PEMFC and methodologies for the development of such tests is presented by Petrone et al. [127]. These methodologies can clearly be of great help in determining their equivalent for electrolysis.

For electrolyzers, Kuhner et al. [29] presents a first approach to a review of the procedure proposed under the name of AST in the literature and Tomic et al. [26] a review of the testing procedures for PEMWE degradation and the need for standardisation and appropriate definition to allow results comparison. In turn, this section reviews the protocols available under this name in the literature for dynamic and steady-state conditions. The protocols are categorized based on the levels suggested by the EU harmonised protocols: cell components, single cell and stack [27].

3.1. Accelerated stress tests for PEMWE cell components

Achieving high electrolysis efficiency with a reduction in the materials prices is one of the main objectives of researchers today, who seek for example to reduce the use of $Pt < 0.2$ $[gr \cdot cm^{-2}]$ and $Ir < 0.3$ $[gr \cdot cm^{-2}]$ [131]. Achieving such performance and cost objectives are mostly based on the proposition of appropriate protocols that allow developments in reasonable periods of time. Accelerated protocols are thus a fundamental building block for the maturity of PEM technology, starting with the development and improvement of new materials for electrolysis cell components. For same aim, this section explores the proposed procedures for electrolysis cell components: membrane, catalysts, MEA, GDL/PTL and bipolar plates.

Although the studies on accelerated protocols for PEM electrolyzers are not numerous, the most common in this group are those proposed for the anode catalyst, mostly based on iridium. In order to obtain data in reduced time on the catalyst stability of the OER, Spöri et al. [132] propose an AST consisting of voltage cycling between 1.75 $[V]$ and OCV, as shown in Fig. 5 (a). The temperature of operation in the electrolyzer is set at 80 $[°C]$ and the voltage is cycled with a dwell interval of 3 $[s]$ for $15,000$ cycles. The researchers found a significant degradation of the anode catalyst in tests performed at > 1.8 $[V]$. Therefore, to limit dissolution during static load tests they suggest AST at 1.6 $[V]$ as a new standard test for accelerated degradation. With the same objective of demonstrating the catalyst stability, an Ir supported Sb-doped SnO_2 this time, Thomassen et al. [56] propose a procedure to evaluate the catalyst dissolution. The AST involves a square-wave current cycle between $0.1 - 1$ $A \cdot cm^{-2}$ for a total of 10 $[min]$ cycling intervals and a test duration of 100 $[h]$. To test the durability of the catalyst on the anodic side, Alia et al. [55] propose for their part a protocol consisting of cycling between $1.45 - 2$ $[V]$ with cycle periods of 1 $[min]$, temperature was set at 80 $[°C]$. In agreement with Spöri et al. [132] the last authors have also concluded that at moderate potentials (1.4 to 1.6 $[V]$) the losses are due to Ir particle growth, whereas at high potentials (> 1.8 $[V]$) the losses are mainly due to catalyst dissolution (see section 2.1.1).

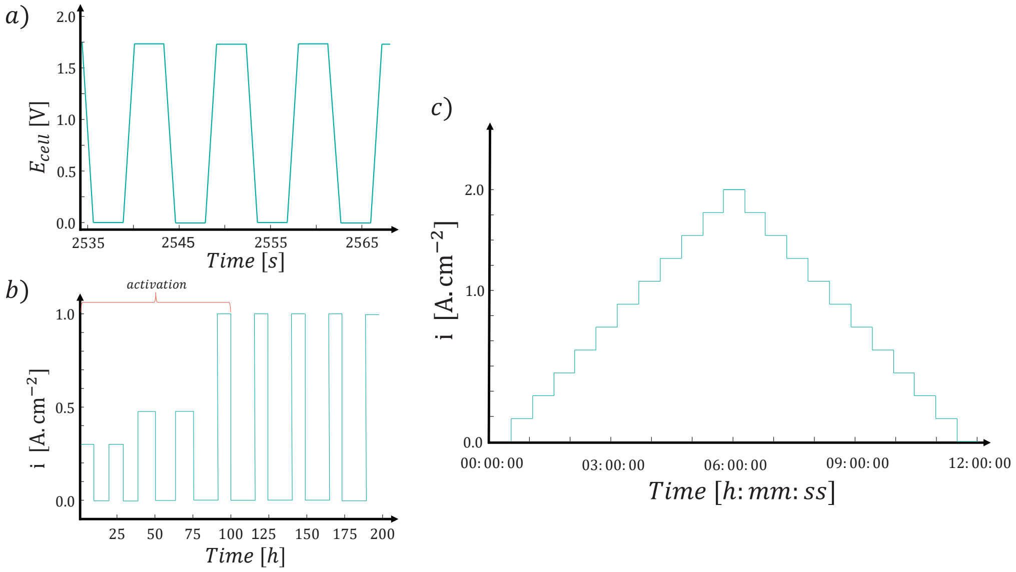

Fig. 5: Accelerated stress test for cell components: a) anode catalyst stability [132], b) MEA testing [77] and c) Anode support catalyst [133]

Since the MEA is seen as the most unstable cell part, some researchers have focused on studying the specific degradation phenomena associated with it. Grigoriev at al. [77] have performed an AST on a MEA, with platinum as catalyst for anode and cathode, by applying galvanostatic pulses. The purpose of the tests is to increase the degradation rate while keeping the cell potential and anode voltage higher than in a conventional cell with Ir as anode catalyst. The proposed protocol presented in Fig. 5 (b) consists of a cycling operation from OCV to 1 $[A \cdot cm^{-2}]$ in 25 $[h]$ cycle periods repeated until the electrolyzer is ruined (stop working). Test was stopped at $5,500$ $[h]$ of electrolyzer operation and the researchers concluded that the first mechanism of MEA degradation is the catalyst layer corrosion with migration of dissolved platinum to the membrane, followed by membrane thinning. Membrane thickness was reduced approximately 75 % during the test. On their side, to compare two different types of Nafion®membranes, Kundu et al. [134] performed accelerated ageing tests for $3-5$ day. In their work, the researchers propose two ex-situ degradation methods consisting of attacking the membrane with OH radicals by a Fenton-type test. The first method consists of introducing the Nafion®membrane into a peroxide and iron solution. The second method is an exchange method in which a sample of Nafion®in the Fe^{2+} form is exposed to a peroxide solution. The Fourier-transform infrared spectroscopy (FTIR) have been obtained for the different membranes by the researchers, showing a clear chemical degradation due to radical's attack.

In order to investigate the usability of micro-sized Ti particles for supporting IrO_2 in the anode of electrolysis cells, Rozain et al. [133] have suggested a specific accelerated test. This protocol, presented in Fig. 5 (c), consists in applying to the cell a series of current steps, with a duration of 30 [min], in a range between 0 and 2 [$A \cdot cm^{-2}$]. The temperature has been set at 80 [$^{\circ}C$]. Additionally the researchers have tested their assembly cell with a real solar energy profile. According to the researchers, the results show evidence of good cell stability with the use of a catalyst composed of only 0.1 [$mg \cdot cm^{-2}$] of IrO_2. This level of performance is obtained thanks to the use of a micro-sized titanium support.

Contrary to the catalytic layers and membrane no studies on accelerated stress test for the Gas Diffusion Layer (GDL) with application to electrolysis have been found in the literature. However, this layer is being investigated for fuel cell applications. For the cathode the GDL can be similar between the two PEM technologies. Then, the proposed protocols for fuel cell can be applied to electrolysis. Chun et al. [135] subjected a GDL accelerated tests in order to research the mechanical degradation of the micro-porous layers in a short period of time. The MPL was subjected to mechanical degradation by applying an AST with a dummy cell for 28 day. Other researchers have focused on studying the accelerated degradation of GDL by applying tests such as electrochemical degradation, freeze/thaw cycles and immersion of this layer in a carbon peroxide solution [117, 136, 137]. For stainless steel GDL, Mo et al. [120] raise the possibility of an accelerated test that can be easily used to investigate the corrosion and durability of various metals by applying high positive voltages intensively at the anode.

3.2. Accelerated stress tests for single cell

Despite the existence of various research on degradation modelling [138, 139] and the development of fuel cell AST, electrolysis cells are not exactly the opposite. Unlike fuel cell, in electrolysis the anode catalysts are mainly IrO_2 and RuO_2 and the membrane is much thicker, which implies a different approach in the analysis of degradation phenomena. Therefore, special care must be taken when transferring concepts from PEMFC modelling to PEMWE applications [90]. For a single electrolysis cell, three protocols have

Stressors	Methodology	Cell component	Ref.
Voltage	Voltage cycling between 1.75 $[V]$ and OCV. Dwell interval of 3 $[s]$ for 15000 cycles. T=80 $[°C]$	Anode catalyst	[132]
Current density	Square-wave current cycle between $0.1-1$ $A{\cdot}cm^{-2}$, 10 $[min]$ cycling intervals and total duration of 100 $[h]$	Anode Catalyst	[56]
Voltage	Cycles between $1.45-2$ $[V]$ with 1 $[min]$ periods.T=80 $[°C]$	Anode catalyst	[55]
Current density	Galvanostatic pulses. Cluces from OCV to 1 $[A \cdot cm^{-2}]$ with 25 $[h]$ periods until the electrolyzer is ruined ($5500h$)	MEA	[77]
Radical attack	Attack the membrane with OH radicals by a Fenton-type test	Membrane	[134]
Current density	Current steps with 30 $[min]$ of duration, from 0 to 2 $[A \cdot cm^{-2}]$. Real solar energy profile applied. $T = 80$ $[°C]$	Anode catalyst	[133]
Mechanical	Mechanical compression applied for 28 days.	GDL	[135]
Voltage	High positive voltages at the anode	GDL (stainless steal)	[120]

Table 2: Summary of cell components AST proposed in state of art for PEMWE

been found in the literature that attempt to evaluate the behaviour of the electrolyzer under real operating conditions, associating operating conditions such as high currents, power fluctuations and periods of inactivity to the degradation mechanisms.

Weiß et al. [95] has proposed an AST that simulates a variable power profile. The cell is powered among high (3 $[A \cdot cm^{-2}]$) and small (0.1 $[A \cdot cm^{-2}]$) current densities, alternating with periods of inactivity during which no current is provided, this protocol is shown in Fig. 6. The principal objective of the test is to assess the impact of electrolysis cells powering from green energies, where operating times and periods of inactivity alternate, for a better understanding of the degradation phenomena. The authors performed an exhaustive electrochemical and physical description of the MEA to understand the changes in cell performance during the applied protocol. Polarisation curves performed during the process revealed that initially there is a growth in performance of 50 $[mV]$ for the first 10 cycles, which is followed by a drop in performance over OCV cycles due to an increase in high-frequency resistance (HFR) of 1.6 times over 718 cycles.

The second protocol has been proposed by Aßmann et al. [140] with the aim of providing a protocol capable of evaluating newly developed materials and components in a short time. The authors believe that the main sources of electrolysis cell degradation are due to high currents, power supply fluctuations and periods of inactivity, and propose a protocol in accordance with these hypotheses. The proposed protocol, presented in Fig. 7, consists of 4 steps: (i) Nominal current density, this is not an intentional stress state, but will lead to some deterioration. (ii) High current density operating: the authors believe that the impact will mainly affect the anode catalyst coating ionomer and the membrane. $Ti-PTL/GDL$ and $Ti-BPP$ will be affected as well if they aren't coated. (iii) Load cycling: this will lead to deterioration of the cathode catalyst. (iv) OCV: regarding the power cycling profile, the major degradation impact will be on cathode side. The researchers propose such a procedure with the aim of determining the degradation rates R_1 to R_4 (Fig. 7) in order to analyse the cell degradation.

Finally, Li et al. [141] have presented a comparative study between 3 single cells tested with different cycling profiles. The first cell taken as a reference is operated at a constant current of 1 $[A \cdot cm^{-2}]$, the second cell is loaded with a dynamic load in the high range, between $1.2-2$ $[A \cdot cm^{-2}]$ and a third cell is cycled at low dynamic loads, between $0-0.5$ $[A \cdot cm^{-2}]$. The researchers found a loss of 29.8 $[\mu V \cdot h^{-1}]$ for the continuous current density

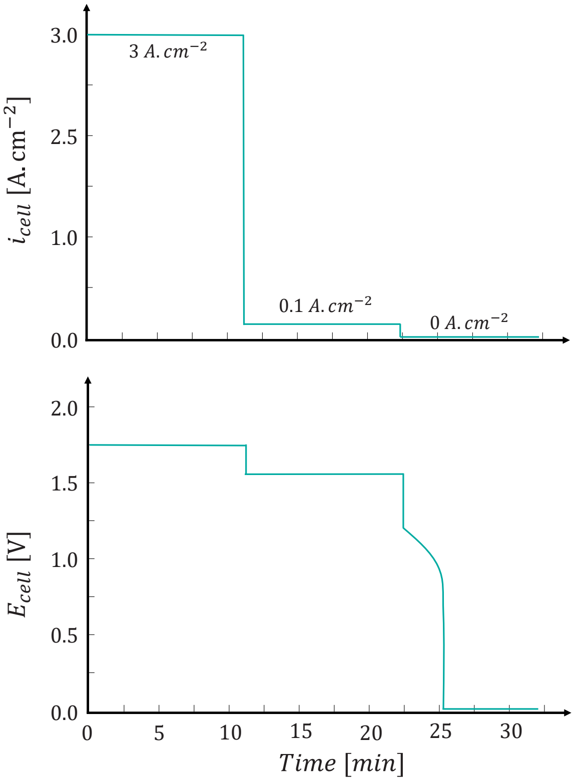

Fig. 6: Accelerated stress test for single cell proposed by [95]

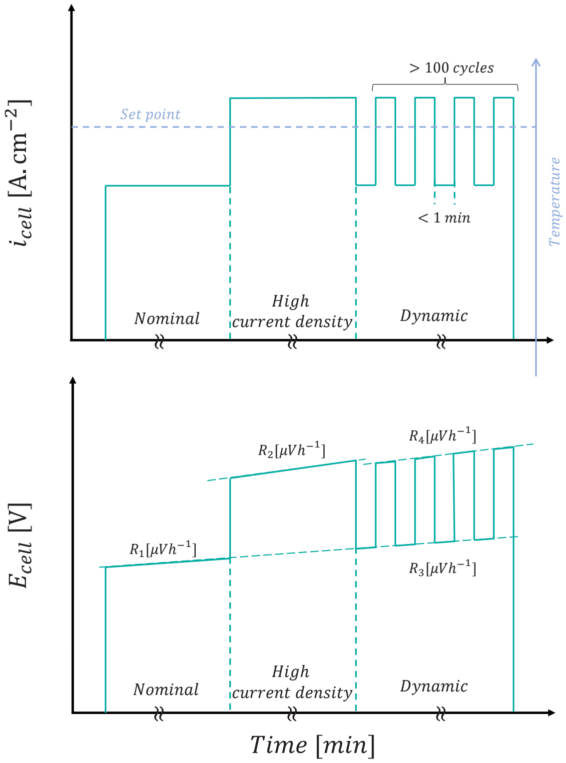

Fig. 7: Accelerated stress test for single cell proposed by [140]

Stressors	Methodology	Ref.
Current density	Power between 3 $[A \cdot cm^{-2}]$ and 0.1 $[A \cdot cm^{-2}]$, followed by OCV period. 718 cycles	[95]
Current density	Nominal period, high current density, load cycling and OCV	[140]
Current density	3 test: constant current density at 1 $[A \cdot cm^{-2}]$, low load cycling $(0 - 0.5\ [A \cdot cm^{-2}])$ and high load cycling $(1.2 - 2\ [A \cdot cm^{-2}])$	[141]

Table 3: Summary of single cell AST proposed in state of art for PEMWE

test, 51.4 $[\mu V \cdot h^{-1}]$ for the low current density cycled test and -55.8 $[\mu V \cdot h^{-1}]$ for the high current density cycled test. In contrast to other investigations in these tests the cell performance worsens at low cycling and improves at high cycling, compared to constant current operation.

3.3. Accelerated stress tests for electrolysis stacks

When stepping from a single cell to a stack, studies on accelerated protocols are rare. At this level Lee et al. [136] propose a protocol for a three-cell stack to evaluate the development and proper functioning of an integrated flexible micro-sensor. This sensor is able to measure current, voltage, flow, pressure and temperature and it can be deployed within the harsh electrochemical electrolysis atmosphere. For manufacturing researchers have used micro-electromechanical systems (MEMS) technology. After evaluating the performance of electrolyzer at different temperatures (> 85 $[°C]$), the authors propose as AST a temperature of 95 $[°C]$ and a high voltage of 3 $[V]$ as test conditions for a 100 $[h]$, as a voltage higher than 3 $[V]$ would damage the catalyst.

4. Test stressors in real electrolysis operation conditions for standard test development

In the last section the available literature on AST/ALT has been discussed from a critical point of view on the need for the development of protocols applicable to real operating conditions. In this section it is presented an analysis for electrolyzers operating conditions as test stressors. Thus, the information available in the literature is presented with a critical overview.

Within an electrolysis stack, six important physical parameters can modify the performance and shorten the electrolyzer lifetime: current density, voltage, pressure, water flow rate, water quality, and temperature [136]. Furthermore, understanding the phenomena of degradation of PEMWE operating under dynamic conditions is essential for the design and implementation of efficient and consistent ways of storing energy from renewable [142]. The aforementioned parameters are also fundamental in the development of control algorithms (i.e., PID, neural network, non-linear, etc.) for renewable energy production and storage systems [98].

From the literature review it was identified that the electrochemical phenomena (see section 2) that cause the performance loss of electrolyzer are directly related to the operating conditions: current density, voltage, temperature, pressure and water flow and quality have important impact on electrolyzer lifetime. As pressure and water quality do not generate a large proportion of degradation phenomena and the latter can be easily avoided with the correct pressure within the operating range of the stack and the treatment of the water to be electrolyzed, these two parameters are not taken into account in this analysis. Therefore, the cycle load (current intensity/voltage), temperature and water flow as stressors for the acceleration of degradation are further discussed in this section. The principal objective of this section is to clearly associate the degradation phenomena presented in section 2 with the operating conditions according to the studies available in the literature. Fig. 8 then presents an overview of the operating modes of electrolysis cells and the associated performance losses, based on state-of-the-art knowledge in order to summarise the analyses developed.

4.1. Cycle load

Power supply is clearly the main operating condition of an electrolysis cell stack because hydrogen production is directly related. Due to the intermittency and fluctuation of the renewable energies with which the electrolyzers are powered for green hydrogen production, it is therefore interesting to evaluate the degradation phenomena that occur in the operating range of voltages for a PEM stack. Several researchers have been interested in analysing the effects of current profiles on the electrolyzers degradation, testing dynamic profiles [46, 93, 112, 143], high and low current densities [89, 144, 145] and start-stop processes [59].

An electrolysis cell can operate at a high current density. While electrolyzers available in market already operate among 0.8 and 2.5 $[A \cdot cm^{-2}]$,

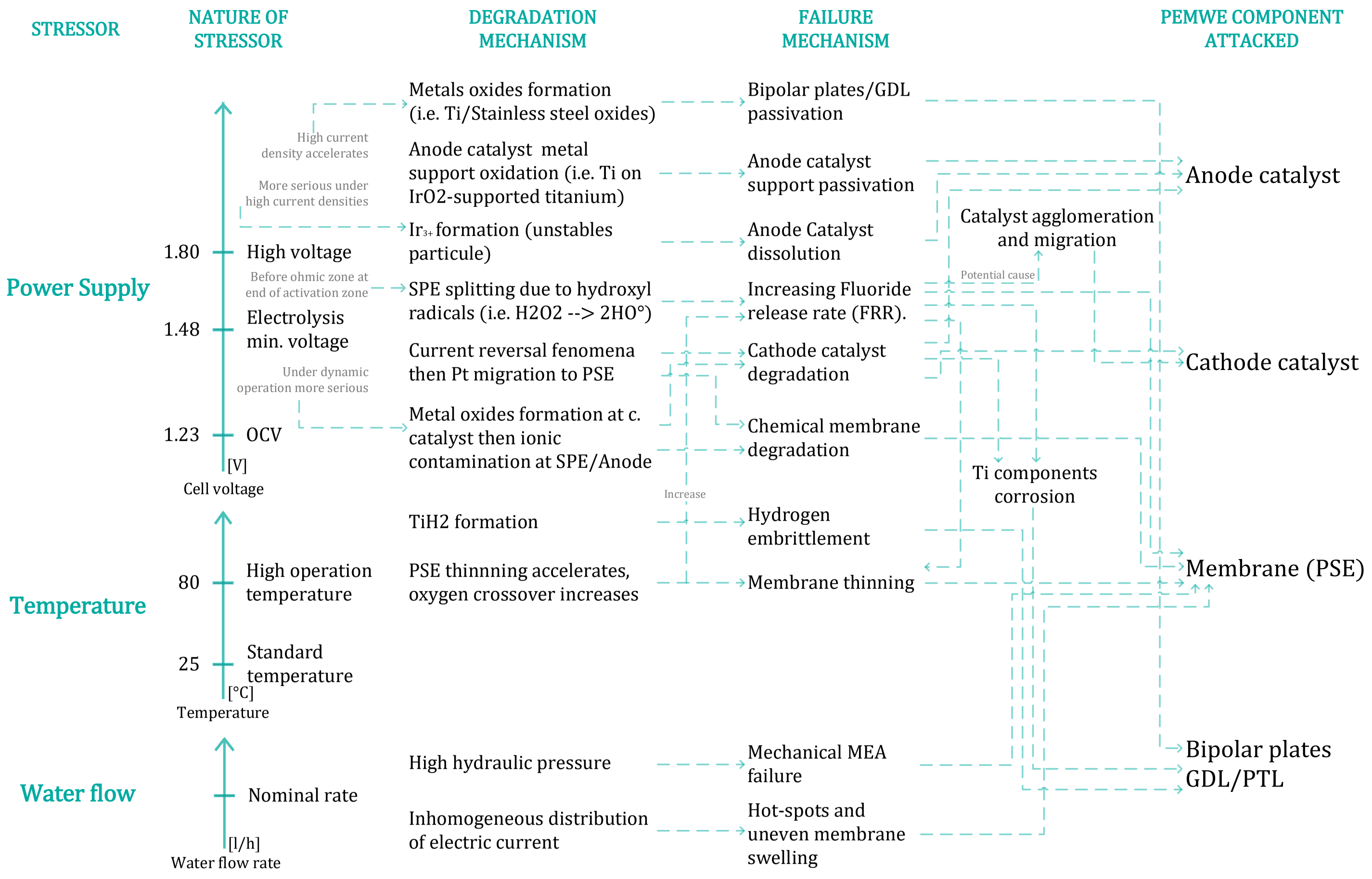

Fig. 8: PEMWE degradation mechanisms associated with operating conditions

laboratory research has taken their performance up to 10 $[A \cdot cm^{-2}]$. The operating voltage, on the other hand, is mainly due to the voltage needed to generate the reaction. The OCV voltage is 1.229 $[V]$, corresponding to the minimum energy needed to generate the breaking of the chemical bonds between hydrogen and oxygen at the anode. The thermoneutral voltage is 1.48 $[V]$, corresponding to the real cell voltage considering that the reaction is endothermic [5]. Finally, it is known from literature that voltages greater than 1.8 $[V]$ accelerate some electrochemical phenomena [132, 142]. The last value is taken as a reference for the operation at high voltages. In the following, the relationships between the different operating ranges of voltage and the electrochemical phenomena, that cause the degradation (see section 2), are established.

4.1.1. Potential between OCV (1.23 $[V]$) *and thermoneutral voltage* (1.48 $[V]$)

Dodwell et al. [59] have shown evidence for a 3-electrode electrolysis cell of degradation phenomena affecting the catalytic layer of the cathode in OCV periods (see 2.1.1). These phenomena thus lead to a performance loss due to membrane contamination and catalyst degradation. The migration of platinum particles can also contaminate the anode catalyst and titanium components. During electrolyzer shutdown processes where the potential can be between the OCV and the thermoneutral minimum potential, Grigoriev et al. [146] have reported the presence of reverse currents. The reverse currents can lead to fuel cell mode operation in which the remaining gases (H_2 and O_2) are consumed. This also leads to the loss of platinum in the catalyst, which is dragged to the areas of the membrane near the cathode. Platinum particles contaminate the membrane and generate a ECSA reduction.

4.1.2. Potential between thermoneutral voltage (1.48 $[V]$*) and high potential* (1.8 $[V]$)

The work of Gubler et al. [97] has established a scientific framework for chemical reactions involving the formation of radicals, exacerbated by the presence of ferrous ions (see section 2.2.1). The kinetic constants of these reactions have also been proposed, which authors Chandesris et al. [90] have taken as a reference for the models development of chemical degradation of the electrolysis membrane. From these studies it has been shown that the chemical reactions that form the radicals are more likely to occur at relatively low current densities. These radicals attack the membrane, leading to the removal of fluorine from the polymer chains. For example, the work of Chandesris et al. [90] shows a maximum fluoride release in the current range $0.4 - 0.5$ $[A \cdot cm^{-2}]$, with an increasing trend before and decreasing trend after, thus forming a negative quadratic behaviour.In terms of voltage, these current densities are found after and close to the thermoneutral potential. This membrane degradation phenomena, evidenced by the release of fluorine, then generates a loss of performance by causing a thinning of the membrane, reducing its effectiveness, and increasing the possibility of gas crossover. Particles shed from the membrane can also degrade the catalyst layers and titanium components.

Other authors such as Weiß et al. [95] also raise the possibility that at low potentials the IrO_2 can be reduced and Ti-based cell parts can corrode. The repeated switching of oxidising and reducing conditions during OCV periods within operation (i.e., among hydrated iridium oxide and metallic iridium) leads to an increase in Ir dissolution.

4.1.3. Potential higher than 1.8 $[V]$

Shirvanian et al. [57] present evidence that at high voltage (> 1.8 $[V]$) the formation of Ir_{III} is enhanced and its instability causes its dissolution in the output water causing a decrease of the catalyst layer and a loss of activity. In addition, authors such as Spöri et al. [62] and Reier et al. [63] have reported the oxidation of the catalyst support, Ti, at high tensions reducing the electrical conductivity.

The harsh operating conditions that generate an oxidising environment (high potential and oxygen presence) have forced the use of materials other than carbon, such as titanium and stainless steel plates, in contrast to fuel cells [121]. However, operation at high potentials (> 1.8 $[V]$) seems to enhance the oxidation of metallic plates. Some researchers have reported the formation of titanium oxides at high operating voltages [95, 110, 112], reducing the electrical conductivity and increasing the contact resistance between the cell layers.

4.1.4. Dynamic and steady-state power supply

The analysis of the degradation associated with the dynamic and steady-state operation is interesting to understand the effect of the coupling with renewable energies, of fluctuating and intermittent nature, on the loss of electrolysis cells performance. Such analysis allows further optimization and robust design of renewable-hydrogen systems [147]. However, among the scientific community, the results seem to differ from one study to another. Rakousky et al. [112] have carried out a comparative study between constant current profiles (1 $[A \cdot cm^{-2}]$, 2 $[A \cdot cm^{-2}]$) and dynamic profiles. Their research concluded that the most degrading profile was the one constant at 2 $[A \cdot cm^{-2}]$, whereas the dynamic profiles applied improve cell degradation. Papakonstantinou et al. [46] have shown no evidence that the dynamic operation has a major influence on degradation. On the other hand, other researchers such as Frensch et al. [93] report that dynamic operation causes a higher rate of fluoride emission and catalyst agglomeration. These processes are then of concern for long-term damage due to membrane thinning that can cause potential gas crossover. Therefore, the debate on PEMWE degradation operated under dynamic profiles provides an important scope for further research.

4.2. Temperature

The operating temperature of the electrolyzer is an important variable in performance. Commercially available stacks have an operating range between $20-70$ $[^{\circ}C]$, whereas theoretically PEMWE can operate in the range of $0-100$ $[^{\circ}C]$ [5]. From the state-of-the-art, it has been identified that although a higher temperature increases the performance of the cell by decreasing the internal resistance, it can also accelerate the degradation of the membrane. Temperatures above 80 $[^{\circ}C]$ as well as low current operation are highly unfavorable in terms of membrane degradation, as the fluoride emission accelerate in such conditions. According to the results presented by Frensch et al. [93], an increment of the temperature from 60 $[^{\circ}C]$ to 80 $[^{\circ}C]$ results in a modest negative effect on the degradation rate, with $1.2-3.0$ $[\mu V \cdot h^{-1}]$ respectively. Whereas operation at 90 $[^{\circ}C]$ had a much more detrimental effect, with 183.8 $[\mu V \cdot h^{-1}]$. Other researchers agree with the conclusion that temperatures above 80 $[^{\circ}C]$ have a negative impact on membrane degradation, accelerating fluoride emission that triggers membrane thinning and increases the probability of gas crossover [21, 94, 148].

It has also been reported that pure titanium suffers from hydrogen embrittled when exposed to temperatures greater than 80 $[^{\circ}C]$. This phenomenon is due to the hydrides formation at grain boundaries [149]. In addition, the pressurised hydrogen generated by the proton reduction reactions on the cathode favours the absorption of hydrogen on the metal bipolar plates, potentially leading to its mechanical deterioration. High temperature is therefore certainly a degrading factor for PEM electrolysis cells. It is suggested for PEMFC that coupling high temperature conditions with different stress cycles is the most suited approach to accelerate the system ageing [127].

4.3. Water flow

In contrast to fuel cells where hydration of the membrane must be of paramount importance to avoid drying phenomena [150], for the electrolyzer this phenomenon is less likely because the membrane is completely submerged in water. However, a water flow that is not adapted to the operating conditions (current intensity and temperature) can cause degradation phenomena such as excess hydraulic pressure or nonuniform distribution of the electric current. Ito et al. [108] present evidence that the type of two-phase flow of circulating water inside the electrolysis cell has important effects on mass transport phenomena. Thus, when the bi-phase circulating water flow at the anode is sluggy or annular, the bulk water transport for the anodic reaction is reduced, and the concentration loss rises at greater current density than when the flow is bubbly. Researchers are also able to analyse the optimal circulating water flow rate on the basis of mass balancing analysis.

Special attention must then be paid to determining the appropriate water flow rate for the operation of the electrolyzers. Excessive water flow increases the hydraulic pressure which can induce mechanical failure of the more fragile elements of the cell, notably the polymeric membrane. At the other extreme, when the water flow is insufficient, temperature can't be controlled optimally, in addition to in-homogeneous current distribution, and the formation of hot spots.

5. Conclusion and perspectives for accelerated degradation testing.

The role of hydrogen in the energy transition is undoubtedly fundamental to achieve the decarbonization objectives set for EU and other energy-intensive regions. The production of hydrogen by proton exchange membrane technology coupling with renewable energies is certainly fundamental. However, it is clear to the scientific community that a considerable improvement of PEMWE is needed to reach a scalability from MW to GW and a marketable price, about 1 [€for kg_{H_2}], as set by DOE and EU.

Three main challenges must be overcome in order to reduce green hydrogen cost by PEM electrolysis through increased reaction efficiency and improved lifetime. First, the development of polymeric membranes that can be operated at temperatures close to 100 [$^{\circ}C$] without accelerating their degradation considerably. Second, the reduction or the replacement of the amount of noble materials used in catalysts while retaining good reaction efficiency. And thirdly, the reduction or elimination of titanium as the main element of GDL/PTL and BPP. To overcome these challenges, it is vital to understand the electrochemical phenomena that cause degradation. This paper presented an extensive literature review of degradation in the polymer membrane, anode and cathode catalysts and multi-phase layers used in PEM electrolysis.

In order to understand the causes of known degradation phenomena, testing under real operating conditions is necessary. Recognising that durability testing is very costly and time-consuming, accelerated testing, which reduces time and cost, is therefore the most interesting approach to increase the understanding of degradation and its causes. This approach is equally interesting for the evaluation of optimisations and new materials, focusing on the achievement of the proposed economic objectives. From a control perspective, accelerated testing can also be very useful in establishing intelligent digital control strategies to optimise the lifetime of the electrolyser.

For electrolysers, unlike fuel cells, accelerated testing has been poorly explored and this article presented evidence of this through a review of existing work. Therefore, AST/ALT have to be developed for electrolysis and obey their own degradation and operating conditions. This work presented a conceptualisation of the operating conditions (power supply, temperature and water flow) and their operating points related to electrochemical phenomena that cause the degradation of materials. This analysis is then the starting point in the methodology of accelerated test development. Future works can choice the stress variables and operation points according to the components or phenomena to be activated. These works should be developed for stacks, allowing to identify the in-homogeneity in cell degradation, and the coupling with renewable, so that they are appropriate to the current needs of the industry.

As mentioned in the introduction of this work, in the authors' understanding an accelerated test is a method that in a reduced time allows to obtain comparable results (degraded components) to the durability test under equivalent operating conditions. The development of this type of methodology should therefore be coupled to this definition, with a view to a future standardisation of the tests and an adequate comparison of the results. This concept is part of the future research lines for PEM electrolysis according to the authors' analysis: development of new materials, privileging the use of non-noble materials, system design and optimisation of control and the development of standardised test protocols.

Acknowledgements

This work has been supported by the EIPHI Graduate School (contract ANR-17- EURE-0002) and the Region Bourgogne Franche-Compté.

References

[1] IPCC, SYNTHESIS REPORT OF THE IPCC SIXTH ASSESSMENT REPORT (AR6), Tech. rep., IPCC (2023).
URL `https://www.ipcc.ch/report/ar6/syr/downloads/report/IPCC_AR6_SYR_LongerReport.pdf`

[2] IEA, CO2 Emissions in 2022 – Analysis, Tech. rep., IEA (2022).
URL `https://www.iea.org/reports/co2-emissions-in-2022`

[3] A. Olabi, M. A. Abdelkareem, Renewable energy and climate change, Renewable and Sustainable Energy Reviews 158 (2022) 112111. `doi:10.1016/j.rser.2022.112111`.
URL `https://linkinghub.elsevier.com/retrieve/pii/S1364032122000405`

[4] IEA, Hydrogen, Tech. rep., IEA (2023).
URL `https://www.iea.org/energy-system/low-emission-fuels/hydrogen`

[5] D. G. Bessarabov, H. Wang, H. Li, N. Zhao (Eds.), PEM electrolysis for hydrogen production: principles and applications, CRC Press, Boca Raton, Florida, 2016, oCLC: ocn930699386.

[6] IEA, Net Zero Emissions by 2050 Scenario (NZE) – Global Energy and Climate Model – Analysis, Tech. rep., IEA (2022).
URL `https://www.iea.org/reports/global-energy-and-climate-model/net-zero-emissions-by-2050-scenario-nze`

[7] I. U. Dedigama, Diagnostics and Modeling of Polymer Electrolyte Membrane Water Electrolysers.

[8] IEA, Global hydrogen production by technology in the Net Zero Scenario, 2019-2030 – Charts – Data & Statistics, Tech. rep., IEA (2022).
URL `https://www.iea.org/data-and-statistics/charts/global-hydrogen-production-by-technology-in-the-net-zero-scenario-2019-2030`

[9] K. Bareiß, C. de la Rua, M. Möckl, T. Hamacher, Life cycle assessment of hydrogen from proton exchange membrane water electrolysis in future energy systems, Applied Energy 237 (2019) 862–872. `doi:10.1016/j.apenergy.2019.01.001`.
URL `https://linkinghub.elsevier.com/retrieve/pii/S0306261919300017`

[10] J. J. Caparrós Mancera, F. Segura Manzano, J. M. Andújar, E. López, F. Isorna, Sun, heat and electricity. A comprehensive study of non-pollutant alternatives to produce green hydrogen, International Journal of Energy Research 46 (13) (2022) 17999–18028. `doi:10.1002/er.8505`.
URL `https://onlinelibrary.wiley.com/doi/10.1002/er.8505`

[11] S. Rosini, S. Germe, F. Fouda-Onana, Les systèmes d'électrolyse de l'eau à membrane échangeuse de protons.

[12] J. Dang, Y. Li, B. Liu, S. Hu, F. Yang, M. Ouyang, Design and economic analysis of high-pressure proton exchange membrane electrolysis for renewable energy storage, International Journal of Hydrogen Energy 48 (28) (2023) 10377–10393. `doi:10.1016/j.ijhydene.2022.11.250`.
URL `https://linkinghub.elsevier.com/retrieve/pii/S0360319922055689`

[13] M. I. Cobo Ángel, C. L. Barraza Botet, N. M. Cantillo Cuello, M. Uribe Laverde (Eds.), Recomendaciones para el desarrollo de la economía del hidrógeno en Colombia: una estrategia nacional de hidrógeno, 1st Edition, Universidad de La Sabana, 2022. `doi:10.5294/978-958-12-0618-6`.
URL `https://publicaciones.unisabana.edu.co/publicaciones/publicaciones/ingenieria/recomendaciones-para-el-desarrollo-de-la-economia-del-hidrogeno-en-colombia/`

[14] EuropeanComission, A hydrogen strategy for a climate-neutral Europe | Knowledge for policy, Tech. Rep. COM/2020/301:, European Comission (2020).
URL `https://knowledge4policy.ec.europa.eu/publication/communication-com2020301-hydrogen-strategy-climate-neutral-europe_en`

[15] W. C. Nadaleti, V. A. Lourenço, G. Americo, Green hydrogen-based pathways and alternatives: Towards the renewable energy transition in South America's regions – Part A, International Journal of Hydrogen Energy 46 (43) (2021) 22247–22255. `doi:10.1016/j.ijhydene.2021.03.239`.
URL `https://linkinghub.elsevier.com/retrieve/pii/S0360319921012350`

[16] W. C. Nadaleti, E. G. de Souza, V. A. Lourenço, Green hydrogen-based pathways and alternatives: Towards the renewable energy transition in South America's regions–Part B, International Journal of Hydrogen Energy 47 (1) (2022) 1–15. `doi:10.1016/j.ijhydene.2021.05.113`.
URL `https://linkinghub.elsevier.com/retrieve/pii/S036031992101867X`

[17] D. Rodríguez-Fontalvo, E. Quiroga, N. M. Cantillo, N. Sánchez, M. Figueredo, M. Cobo, Green hydrogen potential in tropical countries: The colombian case, International Journal of Hydrogen Energy (2023) S0360319923014660`doi:10.1016/j.ijhydene.2023.03.320`.
URL `https://linkinghub.elsevier.com/retrieve/pii/S0360319923014660`

[18] M. N. I. Salehmin, T. Husaini, J. Goh, A. B. Sulong, High-pressure PEM water electrolyser: A review on challenges and mitigation strategies towards green and low-cost hydrogen production, Energy Conversion and Management 268 (2022) 115985. `doi:10.1016/j.enconman.2022.115985`.
URL `https://linkinghub.elsevier.com/retrieve/pii/S0196890422007786`

[19] F. Khatib, T. Wilberforce, O. Ijaodola, E. Ogungbemi, Z. El-Hassan, A. Durrant, J. Thompson, A. Olabi, Material degradation of components in polymer electrolyte membrane (PEM) electrolytic cell and

mitigation mechanisms: A review, Renewable and Sustainable Energy Reviews 111 (2019) 1–14. `doi:10.1016/j.rser.2019.05.007`.
URL `https://linkinghub.elsevier.com/retrieve/pii/S1364032119303132`

[20] O. Schmidt, A. Gambhir, I. Staffell, A. Hawkes, J. Nelson, S. Few, Future cost and performance of water electrolysis: An expert elicitation study, International Journal of Hydrogen Energy 42 (52) (2017) 30470–30492. `doi:10.1016/j.ijhydene.2017.10.045`.
URL `https://linkinghub.elsevier.com/retrieve/pii/S0360319917339435`

[21] S. Siracusano, V. Baglio, N. Van Dijk, L. Merlo, A. S. Aricò, Enhanced performance and durability of low catalyst loading PEM water electrolyser based on a short-side chain perfluorosulfonic ionomer, Applied Energy 192 (2017) 477–489. `doi:10.1016/j.apenergy.2016.09.011`.
URL `https://linkinghub.elsevier.com/retrieve/pii/S0306261916313137`

[22] A. P. R. A. Ferreira, R. C. P. Oliveira, M. M. Mateus, D. M. F. Santos, A Review of the Use of Electrolytic Cells for Energy and Environmental Applications, Energies 16 (4) (2023) 1593. `doi:10.3390/en16041593`.
URL `https://www.mdpi.com/1996-1073/16/4/1593`

[23] Q. Feng, X. Yuan, G. Liu, B. Wei, Z. Zhang, H. Li, H. Wang, A review of proton exchange membrane water electrolysis on degradation mechanisms and mitigation strategies, Journal of Power Sources 366 (2017) 33–55. `doi:10.1016/j.jpowsour.2017.09.006`.
URL `https://linkinghub.elsevier.com/retrieve/pii/S0378775317311631`

[24] U. Babic, M. Suermann, F. N. Büchi, L. Gubler, T. J. Schmidt, Critical Review—Identifying Critical Gaps for Polymer Electrolyte Water Electrolysis Development, Journal of The Electrochemical Society 164 (4) (2017) F387–F399. `doi:10.1149/2.1441704jes`.
URL `https://iopscience.iop.org/article/10.1149/2.1441704jes`

[25] A. Makhsoos, M. Kandidayeni, B. G. Pollet, L. Boulon, A perspective on increasing the efficiency of proton exchange membrane water

electrolyzers– a review, International Journal of Hydrogen Energy 48 (41) (2023) 15341–15370. `doi:10.1016/j.ijhydene.2023.01.048`. URL `https://linkinghub.elsevier.com/retrieve/pii/S0360319923000496`

[26] A. Z. Tomić, I. Pivac, F. Barbir, A review of testing procedures for proton exchange membrane electrolyzer degradation, Journal of Power Sources 557 (2023) 232569. `doi:10.1016/j.jpowsour.2022.232569`. URL `https://linkinghub.elsevier.com/retrieve/pii/S0378775322015464`

[27] G. Tsotridis, A. Pilenga, EU harmonised protocols for testing of low temperature water electrolysers.

[28] F. van der Linden, Methodology and tools for the optimization of the PEM fuel cell break-in procedure, Ph.D. thesis, Université Bourgogne Franche-Comté, Belfort.

[29] E. Kuhnert, V. Hacker, M. Bodner, A Review of Accelerated Stress Tests for Enhancing MEA Durability in PEM Water Electrolysis Cells, International Journal of Energy Research 2023 (2023) 1–23. `doi:10.1155/2023/3183108`.
URL `https://www.hindawi.com/journals/ijer/2023/3183108/`

[30] T. Malkow, A. Pilenga, EU harmonised accelerated stress testing protocols for low-temperature water electrolyser (2024).

[31] G. Chisholm, Chapter 16 - Hydrogen From Water Electrolysis.

[32] B. J. McBride, M. J. Zehe, S. Gordon, NASA Glenn Coefficients for Calculating Thermodynamic Properties of Individual Species (2002).

[33] A. Buttler, H. Spliethoff, Current status of water electrolysis for energy storage, grid balancing and sector coupling via power-to-gas and power-to-liquids: A review, Renewable and Sustainable Energy Reviews 82 (2018) 2440–2454. `doi:10.1016/j.rser.2017.09.003`. URL `https://linkinghub.elsevier.com/retrieve/pii/S136403211731242X`

[34] Z. Kang, H. Wang, Y. Liu, J. Mo, M. Wang, J. Li, X. Tian, Exploring and understanding the internal voltage losses through catalyst layers

in proton exchange membrane water electrolysis devices, Applied Energy 317 (2022) 119213. `doi:10.1016/j.apenergy.2022.119213`.
URL `https://linkinghub.elsevier.com/retrieve/pii/S0306261922005785`

[35] M. Maier, K. Smith, J. Dodwell, G. Hinds, P. Shearing, D. Brett, Mass transport in PEM water electrolysers: A review, International Journal of Hydrogen Energy 47 (1) (2022) 30–56. `doi:10.1016/j.ijhydene.2021.10.013`.
URL `https://linkinghub.elsevier.com/retrieve/pii/S0360319921039288`

[36] D. Falcão, A. Pinto, A review on PEM electrolyzer modelling: Guidelines for beginners, Journal of Cleaner Production 261 (2020) 121184. `doi:10.1016/j.jclepro.2020.121184`.
URL `https://linkinghub.elsevier.com/retrieve/pii/S0959652620312312`

[37] R. García-Valverde, N. Espinosa, A. Urbina, Simple PEM water electrolyser model and experimental validation, International Journal of Hydrogen Energy 37 (2) (2012) 1927–1938. `doi:10.1016/j.ijhydene.2011.09.027`.
URL `https://linkinghub.elsevier.com/retrieve/pii/S0360319911021380`

[38] M. Chatenet, Water electrolysis: from textbook knowledge to the latest scientific strategies and industrial developments, Chem Soc Rev (2022).

[39] N. Danilovic, R. Subbaraman, K.-C. Chang, S. H. Chang, Y. J. Kang, J. Snyder, A. P. Paulikas, D. Strmcnik, Y.-T. Kim, D. Myers, V. R. Stamenkovic, N. M. Markovic, Activity–Stability Trends for the Oxygen Evolution Reaction on Monometallic Oxides in Acidic Environments, The Journal of Physical Chemistry Letters 5 (14) (2014) 2474–2478. `doi:10.1021/jz501061n`.
URL `https://pubs.acs.org/doi/10.1021/jz501061n`

[40] B.-J. Kim, D. F. Abbott, X. Cheng, E. Fabbri, M. Nachtegaal, F. Bozza, I. E. Castelli, D. Lebedev, R. Schäublin, C. Copéret,

T. Graule, N. Marzari, T. J. Schmidt, Unraveling Thermodynamics, Stability, and Oxygen Evolution Activity of Strontium Ruthenium Perovskite Oxide, ACS Catalysis 7 (5) (2017) 3245–3256. `doi:10.1021/acscatal.6b03171`.
URL `https://pubs.acs.org/doi/10.1021/acscatal.6b03171`

[41] A. Hartig-Weiss, M. Miller, H. Beyer, A. Schmitt, A. Siebel, A. T. S. Freiberg, H. A. Gasteiger, H. A. El-Sayed, Iridium Oxide Catalyst Supported on Antimony-Doped Tin Oxide for High Oxygen Evolution Reaction Activity in Acidic Media, ACS Applied Nano Materials 3 (3) (2020) 2185–2196. `doi:10.1021/acsanm.9b02230`.
URL `https://pubs.acs.org/doi/10.1021/acsanm.9b02230`

[42] S. Song, H. Zhang, X. Ma, Z. Shao, R. T. Baker, B. Yi, Electrochemical investigation of electrocatalysts for the oxygen evolution reaction in PEM water electrolyzers, International Journal of Hydrogen Energy 33 (19) (2008) 4955–4961. `doi:10.1016/j.ijhydene.2008.06.039`.
URL `https://linkinghub.elsevier.com/retrieve/pii/S0360319908007520`

[43] M. Bernt, A. Hartig-Weiß, M. F. Tovini, H. A. El-Sayed, C. Schramm, J. Schröter, C. Gebauer, H. A. Gasteiger, Current Challenges in Catalyst Development for PEM Water Electrolyzers, Chemie Ingenieur Technik 92 (1-2) (2020) 31–39. `doi:10.1002/cite.201900101`.
URL `https://onlinelibrary.wiley.com/doi/10.1002/cite.201900101`

[44] M. Bernt, A. Siebel, H. A. Gasteiger, Analysis of Voltage Losses in PEM Water Electrolyzers with Low Platinum Group Metal Loadings, Journal of The Electrochemical Society 165 (5) (2018) F305–F314. `doi:10.1149/2.0641805jes`.
URL `https://iopscience.iop.org/article/10.1149/2.0641805jes`

[45] V. Liso, G. Savoia, S. S. Araya, G. Cinti, S. K. Kær, Modelling and Experimental Analysis of a Polymer Electrolyte Membrane Water Electrolysis Cell at Different Operating Temperatures, Energies 11 (12) (2018) 3273. `doi:10.3390/en11123273`.
URL `http://www.mdpi.com/1996-1073/11/12/3273`

[46] G. Papakonstantinou, G. Algara-Siller, D. Teschner, T. Vidaković-Koch, R. Schlögl, K. Sundmacher, Degradation study of a proton exchange membrane water electrolyzer under dynamic operation conditions, Applied Energy 280 (2020) 115911. `doi:10.1016/j.apenergy.2020.115911`.
URL `https://linkinghub.elsevier.com/retrieve/pii/S0306261920313751`

[47] S. Ramakrishna, D. Srinivasulu Reddy, S. Shiva Kumar, V. Himabindu, Nitrogen doped CNTs supported Palladium electrocatalyst for hydrogen evolution reaction in PEM water electrolyser, International Journal of Hydrogen Energy 41 (45) (2016) 20447–20454. `doi:10.1016/j.ijhydene.2016.08.195`.
URL `https://linkinghub.elsevier.com/retrieve/pii/S0360319916326866`

[48] K.-J. Jeong, Y. Lee, T.-N. Huynh, H. Nersisyan, H. Suh, J. Lee, Liquid-Metal-Assisted Synthesis of Single-Crystalline TiC Nanocubes with Exposed 100 Facets for Enhanced Electrocatalytic Activity in the Hydrogen Evolution Reaction, Small Methods 7 (1) (2023) 2201076, _eprint: https://onlinelibrary.wiley.com/doi/pdf/10.1002/smtd.202201076. `doi:10.1002/smtd.202201076`.
URL `https://onlinelibrary.wiley.com/doi/abs/10.1002/smtd.202201076`

[49] J. Yu, A mini-review of noble-metal-free electrocatalysts for overall water splitting in non-alkaline electrolytes (2021).

[50] N. Yuan, A review on non-noble metal based electrocatalysis for the oxygen evolution reaction.

[51] C. Rozain, E. Mayousse, N. Guillet, P. Millet, Influence of iridium oxide loadings on the performance of PEM water electrolysis cells: Part I–Pure IrO 2 -based anodes, Applied Catalysis B: Environmental 182 (2016) 153–160. `doi:10.1016/j.apcatb.2015.09.013`.
URL `https://linkinghub.elsevier.com/retrieve/pii/S0926337315301399`

[52] S. M. Alia, S. Stariha, R. L. Borup, Electrolyzer Durability at Low Catalyst Loading and with Dynamic Operation, Journal

of The Electrochemical Society 166 (15) (2019) F1164–F1172. `doi:10.1149/2.0231915jes`.
URL `https://iopscience.iop.org/article/10.1149/2.0231915jes`

[53] S. Cherevko, S. Geiger, O. Kasian, A. Mingers, K. J. Mayrhofer, Oxygen evolution activity and stability of iridium in acidic media. Part 2. – Electrochemically grown hydrous iridium oxide, Journal of Electroanalytical Chemistry 774 (2016) 102–110. `doi:10.1016/j.jelechem.2016.05.015`.
URL `https://linkinghub.elsevier.com/retrieve/pii/S1572665716302405`

[54] S. Cherevko, S. Geiger, O. Kasian, A. Mingers, K. J. Mayrhofer, Oxygen evolution activity and stability of iridium in acidic media. Part 1. – Metallic iridium, Journal of Electroanalytical Chemistry 773 (2016) 69–78. `doi:10.1016/j.jelechem.2016.04.033`.
URL `https://linkinghub.elsevier.com/retrieve/pii/S157266571630193X`

[55] S. M. Alia, B. Rasimick, C. Ngo, K. C. Neyerlin, S. S. Kocha, S. Pylypenko, H. Xu, B. S. Pivovar, Activity and Durability of Iridium Nanoparticles in the Oxygen Evolution Reaction, Journal of The Electrochemical Society 163 (11) (2016) F3105–F3112. `doi:10.1149/2.0151611jes`.
URL `https://iopscience.iop.org/article/10.1149/2.0151611jes`

[56] M. S. Thomassen, T. Mokkelbost, E. Sheridan, A. Lind, Supported Nanostructured Ir and IrRu Electrocatalysts for Oxygen Evolution in PEM Electrolysers, ECS Transactions 35 (34) (2011) 271, publisher: IOP Publishing. `doi:10.1149/1.3654225`.
URL `https://iopscience.iop.org/article/10.1149/1.3654225/meta`

[57] P. Shirvanian, F. van Berkel, Novel components in Proton Exchange Membrane (PEM) Water Electrolyzers (PEMWE): Status, challenges and future needs. A mini review, Electrochemistry Communications 114 (2020) 106704. `doi:10.1016/j.elecom.2020.106704`.

URL https://linkinghub.elsevier.com/retrieve/pii/S1388248120300552

[58] O. Panchenko, M. Carmo, M. Rasinski, T. Arlt, I. Manke, M. Müller, W. Lehnert, Non-destructive in-operando investigation of catalyst layer degradation for water electrolyzers using synchrotron radiography, Materials Today Energy 16 (2020) 100394. doi:10.1016/j.mtener.2020.100394.
URL https://linkinghub.elsevier.com/retrieve/pii/S2468606920300137

[59] J. Dodwell, M. Maier, J. Majasan, R. Jervis, L. Castanheira, P. Shearing, G. Hinds, D. Brett, Open-circuit dissolution of platinum from the cathode in polymer electrolyte membrane water electrolysers, Journal of Power Sources 498 (2021) 229937. doi:10.1016/j.jpowsour.2021.229937.
URL https://linkinghub.elsevier.com/retrieve/pii/S0378775321004699

[60] H. Su, M. A. Soldatov, V. Roldugin, Q. Liu, Platinum single-atom catalyst with self-adjustable valence state for large-current-density acidic water oxidation, eScience 2 (1) (2022) 102–109. doi:10.1016/j.esci.2021.12.007.
URL https://linkinghub.elsevier.com/retrieve/pii/S2667141721000549

[61] E. Brightman, J. Dodwell, N. van Dijk, G. Hinds, In situ characterisation of PEM water electrolysers using a novel reference electrode, Electrochemistry Communications 52 (2015) 1–4. doi:10.1016/j.elecom.2015.01.005.
URL https://linkinghub.elsevier.com/retrieve/pii/S1388248115000065

[62] C. Spöri, J. T. H. Kwan, A. Bonakdarpour, D. P. Wilkinson, P. Strasser, The Stability Challenges of Oxygen Evolving Catalysts: Towards a Common Fundamental Understanding and Mitigation of Catalyst Degradation, Angewandte Chemie International Edition 56 (22) (2017) 5994–6021. doi:10.1002/anie.201608601.
URL https://onlinelibrary.wiley.com/doi/10.1002/anie.201608601

[63] T. Reier, D. Teschner, T. Lunkenbein, A. Bergmann, S. Selve, R. Kraehnert, R. Schlögl, P. Strasser, Electrocatalytic Oxygen Evolution on Iridium Oxide: Uncovering Catalyst-Substrate Interactions and Active Iridium Oxide Species, Journal of The Electrochemical Society 161 (9) (2014) F876–F882. `doi:10.1149/2.0411409jes`.
URL `https://iopscience.iop.org/article/10.1149/2.0411409jes`

[64] P. Lettenmeier, R. Wang, R. Abouatallah, S. Helmly, T. Morawietz, R. Hiesgen, S. Kolb, F. Burggraf, J. Kallo, A. Gago, K. Friedrich, Durable Membrane Electrode Assemblies for Proton Exchange Membrane Electrolyzer Systems Operating at High Current Densities, Electrochimica Acta 210 (2016) 502–511. `doi:10.1016/j.electacta.2016.04.164`.
URL `https://linkinghub.elsevier.com/retrieve/pii/S0013468616310167`

[65] C. Rakousky, U. Reimer, K. Wippermann, M. Carmo, W. Lueke, D. Stolten, An analysis of degradation phenomena in polymer electrolyte membrane water electrolysis, Journal of Power Sources 326 (2016) 120–128. `doi:10.1016/j.jpowsour.2016.06.082`.
URL `https://linkinghub.elsevier.com/retrieve/pii/S0378775316307844`

[66] S. Shrestha, Y. Liu, W. E. Mustain, Electrocatalytic Activity and Stability of Pt clusters on State-of-the-Art Supports: A Review, Catalysis Reviews 53 (3) (2011) 256–336. `doi:10.1080/01614940.2011.596430`.
URL `http://www.tandfonline.com/doi/abs/10.1080/01614940.2011.596430`

[67] F. Claudel, L. Dubau, G. Berthomé, L. Sola-Hernandez, C. Beauger, L. Piccolo, F. Maillard, Degradation Mechanisms of Oxygen Evolution Reaction Electrocatalysts: A Combined Identical-Location Transmission Electron Microscopy and X-ray Photoelectron Spectroscopy Study, ACS Catalysis 9 (5) (2019) 4688–4698. `doi:10.1021/acscatal.9b00280`.
URL `https://pubs.acs.org/doi/10.1021/acscatal.9b00280`

[68] D. Santos, A. Lopes, M. J. Pacheco, A. Gomes, L. Ciríaco, The Oxygen Evolution Reaction at Sn-Sb Oxide Anodes: Influence of the

Oxide Preparation Mode, Journal of The Electrochemical Society 161 (9) (2014) H564–H572. `doi:10.1149/2.1031409jes`.
URL `https://iopscience.iop.org/article/10.1149/2.1031409jes`

[69] J. Polonský, P. Mazúr, M. Paidar, E. Christensen, K. Bouzek, Performance of a PEM water electrolyser using a TaC-supported iridium oxide electrocatalyst, International Journal of Hydrogen Energy 39 (7) (2014) 3072–3078. `doi:10.1016/j.ijhydene.2013.12.085`.
URL `https://linkinghub.elsevier.com/retrieve/pii/S0360319913030206`

[70] P. Paciok, M. Carmo, W. Lüke, M. Heggen, D. Stolten, Investigation of Pt/C Catalysts Using Identical Location Transmission Electron Microscopy Under PEM Electrolysis Conditions, ECS Meeting Abstracts MA2016-02 (38) (2016) 2505–2505. `doi:10.1149/MA2016-02/38/2505`.
URL `https://iopscience.iop.org/article/10.1149/MA2016-02/38/2505`

[71] X. Wang, L. Zhang, G. Li, G. Zhang, Z.-G. Shao, B. Yi, The influence of Ferric ion contamination on the solid polymer electrolyte water electrolysis performance, Electrochimica Acta 158 (2015) 253–257. `doi:10.1016/j.electacta.2015.01.140`.
URL `https://linkinghub.elsevier.com/retrieve/pii/S0013468615001863`

[72] P. Millet, R. Ngameni, S. Grigoriev, N. Mbemba, F. Brisset, A. Ranjbari, C. Etiévant, PEM water electrolyzers: From electrocatalysis to stack development, International Journal of Hydrogen Energy 35 (10) (2010) 5043–5052. `doi:10.1016/j.ijhydene.2009.09.015`.
URL `https://linkinghub.elsevier.com/retrieve/pii/S036031990901386X`

[73] C. Rakousky, G. P. Keeley, K. Wippermann, M. Carmo, D. Stolten, The stability challenge on the pathway to high-current-density polymer electrolyte membrane water electrolyzers, Electrochimica Acta 278 (2018) 324–331. `doi:10.1016/j.electacta.2018.04.154`.
URL `https://www.sciencedirect.com/science/article/pii/S0013468618309150`

[74] G. Wei, Y. Wang, C. Huang, Q. Gao, Z. Wang, L. Xu, The stability of MEA in SPE water electrolysis for hydrogen production, International Journal of Hydrogen Energy 35 (9) (2010) 3951–3957. `doi:10.1016/j.ijhydene.2010.01.153`.
URL `https://linkinghub.elsevier.com/retrieve/pii/S0360319910002648`

[75] S. Sun, Z. Shao, H. Yu, G. Li, B. Yi, Investigations on degradation of the long-term proton exchange membrane water electrolysis stack, Journal of Power Sources 267 (2014) 515–520. `doi:10.1016/j.jpowsour.2014.05.117`.
URL `https://linkinghub.elsevier.com/retrieve/pii/S0378775314008106`

[76] M. Pan, C. Pan, C. Li, J. Zhao, A review of membranes in proton exchange membrane fuel cells: Transport phenomena, performance and durability, Renewable and Sustainable Energy Reviews 141 (2021) 110771. `doi:10.1016/j.rser.2021.110771`.
URL `https://linkinghub.elsevier.com/retrieve/pii/S1364032121000666`

[77] S. Grigoriev, K. Dzhus, D. Bessarabov, P. Millet, Failure of PEM water electrolysis cells: Case study involving anode dissolution and membrane thinning, International Journal of Hydrogen Energy 39 (35) (2014) 20440–20446. `doi:10.1016/j.ijhydene.2014.05.043`.
URL `https://linkinghub.elsevier.com/retrieve/pii/S0360319914013913`

[78] A. Z. Al Munsur, B.-H. Goo, Y. Kim, O. J. Kwon, S. Y. Paek, S. Y. Lee, H.-J. Kim, T.-H. Kim, Nafion-Based Proton-Exchange Membranes Built on Cross-Linked Semi-Interpenetrating Polymer Networks between Poly(acrylic acid) and Poly(vinyl alcohol), ACS Applied Materials & Interfaces 13 (24) (2021) 28188–28200. `doi:10.1021/acsami.1c05662`.
URL `https://pubs.acs.org/doi/10.1021/acsami.1c05662`

[79] G.-B. Jung, S.-H. Chan, C.-J. Lai, C.-C. Yeh, J.-W. Yu, Innovative Membrane Electrode Assembly (MEA) Fabrication for Proton Exchange Membrane Water Electrolysis, Energies 12 (21) (2019) 4218.

doi:10.3390/en12214218.
URL https://www.mdpi.com/1996-1073/12/21/4218

[80] K. Song, Y. Wang, Y. Ding, H. Xu, P. Mueller-Welt, T. Stuermlinger, K. Bause, C. Ehrmann, H. W. Weinmann, J. Schaefer, J. Fleischer, K. Zhu, F. Weihard, M. Trostmann, M. Schwartze, A. Albers, Assembly techniques for proton exchange membrane fuel cell stack: A literature review, Renewable and Sustainable Energy Reviews 153 (2022) 111777. doi:10.1016/j.rser.2021.111777.
URL https://linkinghub.elsevier.com/retrieve/pii/S1364032121010467

[81] K. Talukdar, P. Gazdzicki, K. A. Friedrich, Comparative investigation into the performance and durability of long and short side chain ionomers in Polymer Electrolyte Membrane Fuel Cells, Journal of Power Sources 439 (2019) 227078. doi:10.1016/j.jpowsour.2019.227078.
URL https://linkinghub.elsevier.com/retrieve/pii/S0378775319310717

[82] S. H. Kwon, H. Kang, J. H. Lee, S. Shim, J. Lee, D. S. Lee, C. M. Kim, S. G. Lee, Investigating the influence of the side-chain pendants of perfluorosulfonic acid membranes in a PEMFC by molecular dynamics simulations, Materials Today Communications 21 (2019) 100625. doi:10.1016/j.mtcomm.2019.100625.
URL https://linkinghub.elsevier.com/retrieve/pii/S2352492819306841

[83] S. Giancola, M. Zatoń, Reyes-Carmona, M. Dupont, A. Donnadio, S. Cavaliere, J. Rozière, D. J. Jones, Composite short side chain PFSA membranes for PEM water electrolysis, Journal of Membrane Science 570-571 (2019) 69–76. doi:10.1016/j.memsci.2018.09.063.
URL https://linkinghub.elsevier.com/retrieve/pii/S0376738818308275

[84] O. N. Primachenko, E. A. Marinenko, A. S. Odinokov, S. V. Kononova, Y. V. Kulvelis, V. T. Lebedev, State of the art and prospects in the development of proton-conducting perfluorinated membranes with short side chains: A review, Polymers for Advanced Technologies 32 (4)

(2021) 1386–1408. `doi:10.1002/pat.5191`.
URL `https://onlinelibrary.wiley.com/doi/10.1002/pat.5191`

[85] R. Alink, D. Gerteisen, M. Oszcipok, Degradation effects in polymer electrolyte membrane fuel cell stacks by sub-zero operation—An in situ and ex situ analysis, Journal of Power Sources 182 (1) (2008) 175–187. `doi:10.1016/j.jpowsour.2008.03.074`.
URL `https://linkinghub.elsevier.com/retrieve/pii/S0378775308006113`

[86] J. Aubry, Diagnostic, pronostic, contrôle tolérant aux défauts et au vieillissement d'une pile à combustible à membrane échangeuse de protons, appliqués à l'automobile, Ph.D. thesis, Université Bourgogne Franche-Comté, Belfort.

[87] C. Lorenzo, Méthodologie et outils pour l'optimisation multicritères d'une architecture de train hybride électrique à hydrogène, Ph.D. thesis.

[88] R. M.H. Khorasany, A. Sadeghi Alavijeh, E. Kjeang, G. Wang, R. Rajapakse, Mechanical degradation of fuel cell membranes under fatigue fracture tests, Journal of Power Sources 274 (2015) 1208–1216. `doi:10.1016/j.jpowsour.2014.10.135`.
URL `https://linkinghub.elsevier.com/retrieve/pii/S0378775314017546`

[89] S. Siracusano, S. Trocino, N. Briguglio, F. Pantò, A. S. Aricò, Analysis of performance degradation during steady-state and load-thermal cycles of proton exchange membrane water electrolysis cells, Journal of Power Sources 468 (2020) 228390. `doi:10.1016/j.jpowsour.2020.228390`.
URL `https://linkinghub.elsevier.com/retrieve/pii/S0378775320306947`

[90] M. Chandesris, V. Médeau, N. Guillet, S. Chelghoum, D. Thoby, F. Fouda-Onana, Numerical modelling of membrane degradation in PEM water electrolyzer: Influence of the temperature and current density (2015).

[91] A. Albert, T. Lochner, T. J. Schmidt, L. Gubler, Stability and Degradation Mechanisms of Radiation-Grafted Polymer Electrolyte Membranes for Water Electrolysis, ACS Applied Materials & Interfaces 8 (24) (2016) 15297–15306. `doi:10.1021/acsami.6b03050`.
URL `https://pubs.acs.org/doi/10.1021/acsami.6b03050`

[92] K. E. Ayers, E. Anderson, C. B. Capuano, M. Niedzwiecki, J. Renner, Proton Exchange Membranes for Hydrogen Generation - A Tutorial On Research Needs and Challenges for PEM Electrolysis Vs. Fuel Cells, ECS Meeting Abstracts MA2013-01 (42) (2013) 1440–1440. `doi:10.1149/MA2013-01/42/1440`.
URL `https://iopscience.iop.org/article/10.1149/MA2013-01/42/1440`

[93] S. H. Frensch, F. Fouda-Onana, G. Serre, D. Thoby, S. S. Araya, S. K. Kær, Influence of the operation mode on PEM water electrolysis degradation, International Journal of Hydrogen Energy 44 (57) (2019) 29889–29898. `doi:10.1016/j.ijhydene.2019.09.169`.
URL `https://linkinghub.elsevier.com/retrieve/pii/S036031991933592X`

[94] F. Fouda-Onana, M. Chandesris, V. Médeau, S. Chelghoum, D. Thoby, N. Guillet, Investigation on the degradation of MEAs for PEM water electrolysers part I: Effects of testing conditions on MEA performances and membrane properties, International Journal of Hydrogen Energy 41 (38) (2016) 16627–16636. `doi:10.1016/j.ijhydene.2016.07.125`.
URL `https://linkinghub.elsevier.com/retrieve/pii/S0360319916321164`

[95] A. Weiß, A. Siebel, M. Bernt, T.-H. Shen, V. Tileli, H. A. Gasteiger, Impact of Intermittent Operation on Lifetime and Performance of a PEM Water Electrolyzer, Journal of The Electrochemical Society 166 (8) (2019) F487–F497. `doi:10.1149/2.0421908jes`.
URL `https://iopscience.iop.org/article/10.1149/2.0421908jes`

[96] S. H. Frensch, G. Serre, F. Fouda-Onana, H. C. Jensen, M. L. Christensen, S. S. Araya, S. K. Kær, Impact of iron and hydrogen peroxide on membrane degradation for polymer electrolyte membrane

water electrolysis: Computational and experimental investigation on fluoride emission, Journal of Power Sources 420 (2019) 54–62. `doi:10.1016/j.jpowsour.2019.02.076`.
URL `https://linkinghub.elsevier.com/retrieve/pii/S0378775319302010`

[97] L. Gubler, S. M. Dockheer, W. H. Koppenol, Radical (HO • , H • and HOO •) Formation and Ionomer Degradation in Polymer Electrolyte Fuel Cells, Journal of The Electrochemical Society 158 (7) (2011) B755–B769. `doi:10.1149/1.3581040`.
URL `https://iopscience.iop.org/article/10.1149/1.3581040`

[98] A. Majumdar, M. Haas, I. Elliot, S. Nazari, Control and control-oriented modeling of PEM water electrolyzers: A review, International Journal of Hydrogen Energy (2023) S0360319923019882`doi:10.1016/j.ijhydene.2023.04.204`.
URL `https://linkinghub.elsevier.com/retrieve/pii/S0360319923019882`

[99] B. Bensmann, R. Hanke-Rauschenbach, K. Sundmacher, In-situ measurement of hydrogen crossover in polymer electrolyte membrane water electrolysis, International Journal of Hydrogen Energy 39 (1) (2014) 49–53. `doi:10.1016/j.ijhydene.2013.10.085`.
URL `https://linkinghub.elsevier.com/retrieve/pii/S0360319913025974`

[100] P. Trinke, B. Bensmann, S. Reichstein, R. Hanke-Rauschenbach, K. Sundmacher, Hydrogen Permeation in PEM Electrolyzer Cells Operated at Asymmetric Pressure Conditions, Journal of The Electrochemical Society 163 (11) (2016) F3164–F3170. `doi:10.1149/2.0221611jes`.
URL `https://iopscience.iop.org/article/10.1149/2.0221611jes`

[101] K. E. Ayers, E. B. Anderson, C. Capuano, B. Carter, L. Dalton, G. Hanlon, J. Manco, M. Niedzwiecki, Research Advances towards Low Cost, High Efficiency PEM Electrolysis, ECS Transactions 33 (1) (2010) 3–15. `doi:10.1149/1.3484496`.
URL `https://iopscience.iop.org/article/10.1149/1.3484496`

[102] C. A. Wilkie, J. R. Thomsen, M. L. Mittleman, Interaction of poly(methyl methacrylate) and nafions, Journal of Applied Polymer Science 42 (4) (1991) 901–909. `doi:10.1002/app.1991.070420404`.
URL `https://onlinelibrary.wiley.com/doi/10.1002/app.1991.070420404`

[103] J. Zhao, X. Li, A review of polymer electrolyte membrane fuel cell durability for vehicular applications: Degradation modes and experimental techniques, Energy Conversion and Management 199 (2019) 112022. `doi:10.1016/j.enconman.2019.112022`.
URL `https://linkinghub.elsevier.com/retrieve/pii/S0196890419310283`

[104] Q. Yan, H. Toghiani, Y.-W. Lee, K. Liang, H. Causey, Effect of sub-freezing temperatures on a PEM fuel cell performance, startup and fuel cell components, Journal of Power Sources 160 (2) (2006) 1242–1250. `doi:10.1016/j.jpowsour.2006.02.075`.
URL `https://linkinghub.elsevier.com/retrieve/pii/S037877530600382X`

[105] P. Millet, A. Ranjbari, F. de Guglielmo, S. Grigoriev, F. Auprêtre, Cell failure mechanisms in PEM water electrolyzers, International Journal of Hydrogen Energy 37 (22) (2012) 17478–17487. `doi:10.1016/j.ijhydene.2012.06.017`.
URL `https://linkinghub.elsevier.com/retrieve/pii/S0360319912013638`

[106] S. Grigoriev, V. Porembskiy, S. Korobtsev, V. Fateev, F. Auprêtre, P. Millet, High-pressure PEM water electrolysis and corresponding safety issues, International Journal of Hydrogen Energy 36 (3) (2011) 2721–2728. `doi:10.1016/j.ijhydene.2010.03.058`.
URL `https://linkinghub.elsevier.com/retrieve/pii/S0360319910005392`

[107] S. Grigoriev, P. Millet, S. Korobtsev, V. Porembskiy, M. Pepic, C. Etievant, C. Puyenchet, V. Fateev, Hydrogen safety aspects related to high-pressure polymer electrolyte membrane water electrolysis, International Journal of Hydrogen Energy 34 (14) (2009) 5986–5991. `doi:10.1016/j.ijhydene.2009.01.047`.

URL https://linkinghub.elsevier.com/retrieve/pii/S0360319909001219

[108] H. Ito, T. Maeda, A. Nakano, Y. Hasegawa, N. Yokoi, C. Hwang, M. Ishida, A. Kato, T. Yoshida, Effect of flow regime of circulating water on a proton exchange membrane electrolyzer, International Journal of Hydrogen Energy 35 (18) (2010) 9550–9560. `doi:10.1016/j.ijhydene.2010.06.103`.
URL https://linkinghub.elsevier.com/retrieve/pii/S036031991001284X

[109] F. Lapicque, M. Belhadj, C. Bonnet, J. Pauchet, Y. Thomas, A critical review on gas diffusion micro and macroporous layers degradations for improved membrane fuel cell durability, Journal of Power Sources 336 (2016) 40–53. `doi:10.1016/j.jpowsour.2016.10.037`.
URL https://linkinghub.elsevier.com/retrieve/pii/S037877531631429X

[110] M. Prestat, Corrosion of structural components of proton exchange membrane water electrolyzer anodes: A review, Journal of Power Sources 556 (2023) 232469. `doi:10.1016/j.jpowsour.2022.232469`.
URL https://linkinghub.elsevier.com/retrieve/pii/S037877532201446X

[111] C. Liu, M. Shviro, G. Bender, A. S. Gago, T. Morawietz, M. Dzara, I. Biswas, P. Gazdzicki, Z. Kang, S. Zaccarine, S. Pylypenko, K. A. Friedrich, M. Carmo, W. Lehnert, Degradation Effects at the Porous Transport Layer/Catalyst Layer Interface in Polymer Electrolyte Membrane Water Electrolyzer, Journal of The Electrochemical Society (Mar. 2023). `doi:10.1149/1945-7111/acc1a5`.
URL https://iopscience.iop.org/article/10.1149/1945-7111/acc1a5

[112] C. Rakousky, U. Reimer, K. Wippermann, S. Kuhri, M. Carmo, W. Lueke, D. Stolten, Polymer electrolyte membrane water electrolysis: Restraining degradation in the presence of fluctuating power, Journal of Power Sources 342 (2017) 38–47. `doi:10.1016/j.jpowsour.2016.11.118`.
URL https://linkinghub.elsevier.com/retrieve/pii/S0378775316316858

[113] T. Bystron, M. Vesely, M. Paidar, G. Papakonstantinou, K. Sundmacher, B. Bensmann, R. Hanke-Rauschenbach, K. Bouzek, Enhancing PEM water electrolysis efficiency by reducing the extent of Ti gas diffusion layer passivation, Journal of Applied Electrochemistry 48 (6) (2018) 713–723. `doi:10.1007/s10800-018-1174-6`.
URL `http://link.springer.com/10.1007/s10800-018-1174-6`

[114] A. Gago, S. Ansar, B. Saruhan, U. Schulz, P. Lettenmeier, N. Cañas, P. Gazdzicki, T. Morawietz, R. Hiesgen, J. Arnold, K. Friedrich, Protective coatings on stainless steel bipolar plates for proton exchange membrane (PEM) electrolysers, Journal of Power Sources 307 (2016) 815–825. `doi:10.1016/j.jpowsour.2015.12.071`.
URL `https://linkinghub.elsevier.com/retrieve/pii/S0378775315306832`

[115] P. W. T. Lu, S. Srinivasan, Advances in water electrolysis technology with emphasis on use of the solid polymer electrolyte, Journal of Applied Electrochemistry 9 (3) (1979) 269–283. `doi:10.1007/BF01112480`.
URL `https://doi.org/10.1007/BF01112480`

[116] M. Bierling, D. McLaughlin, B. Mayerhöfer, S. Thiele, Toward Understanding Catalyst Layer Deposition Processes and Distribution in Anodic Porous Transport Electrodes in Proton Exchange Membrane Water Electrolyzers, Advanced Energy Materials 13 (13) (2023) 2203636. `doi:10.1002/aenm.202203636`.
URL `https://onlinelibrary.wiley.com/doi/10.1002/aenm.202203636`

[117] G. Chen, H. Zhang, H. Ma, H. Zhong, Electrochemical durability of gas diffusion layer under simulated proton exchange membrane fuel cell conditions, International Journal of Hydrogen Energy 34 (19) (2009) 8185–8192. `doi:10.1016/j.ijhydene.2009.07.085`.
URL `https://linkinghub.elsevier.com/retrieve/pii/S0360319909011392`

[118] B. Verdin, F. Fouda-Onana, S. Germe, G. Serre, P. Jacques, P. Millet, Operando current mapping on PEM water electrolysis cells. Influence of mechanical stress, International Journal of Hydrogen Energy 42 (41)

(2017) 25848–25859. `doi:10.1016/j.ijhydene.2017.08.189`.
URL `https://linkinghub.elsevier.com/retrieve/pii/S0360319917334924`

[119] C. Lee, W. Mérida, Gas diffusion layer durability under steady-state and freezing conditions, Journal of Power Sources 164 (1) (2007) 141–153. `doi:10.1016/j.jpowsour.2006.09.092`.
URL `https://linkinghub.elsevier.com/retrieve/pii/S0378775306021318`

[120] J. Mo, S. M. Steen, F.-Y. Zhang, T. J. Toops, M. P. Brady, J. B. Green, Electrochemical investigation of stainless steel corrosion in a proton exchange membrane electrolyzer cell, International Journal of Hydrogen Energy 40 (36) (2015) 12506–12511. `doi:10.1016/j.ijhydene.2015.07.061`.
URL `https://www.sciencedirect.com/science/article/pii/S0360319915018340`

[121] H.-Y. Jung, S.-Y. Huang, P. Ganesan, B. N. Popov, Performance of gold-coated titanium bipolar plates in unitized regenerative fuel cell operation, Journal of Power Sources 194 (2) (2009) 972–975. `doi:10.1016/j.jpowsour.2009.06.030`.
URL `https://linkinghub.elsevier.com/retrieve/pii/S0378775309010441`

[122] G. Liu, F. Hou, X. Wang, B. Fang, Conductive Polymer and Nanoparticle-Promoted Polymer Hybrid Coatings for Metallic Bipolar Plates in Proton Membrane Exchange Water Electrolysis, Applied Sciences 13 (3) (2023) 1244. `doi:10.3390/app13031244`.
URL `https://www.mdpi.com/2076-3417/13/3/1244`

[123] X. Luo, C. Ren, J. Song, H. Luo, K. Xiao, D. Zhang, J. Hao, Z. Deng, C. Dong, X. Li, Design and fabrication of bipolar plates for PEM water electrolyser, Journal of Materials Science & Technology 146 (2023) 19–41. `doi:10.1016/j.jmst.2022.10.039`.
URL `https://linkinghub.elsevier.com/retrieve/pii/S1005030222008635`

[124] S. S. Dihrab, K. Sopian, M. A. Alghoul, M. Y. Sulaiman, Review of the membrane and bipolar plates materials for conventional and unitized

regenerative fuel cells, Renewable and Sustainable Energy Reviews 13 (6) (2009) 1663–1668. `doi:10.1016/j.rser.2008.09.029`.
URL `https://www.sciencedirect.com/science/article/pii/S1364032108001676`

[125] M. Zhang, L. Hu, G. Lin, Z. Shao, Honeycomb-like nanocomposite Ti-Ag-N films prepared by pulsed bias arc ion plating on titanium as bipolar plates for unitized regenerative fuel cells, Journal of Power Sources 198 (2012) 196–202. `doi:10.1016/j.jpowsour.2011.10.022`.
URL `https://www.sciencedirect.com/science/article/pii/S0378775311019719`

[126] H.-Y. Jung, S.-Y. Huang, B. N. Popov, High-durability titanium bipolar plate modified by electrochemical deposition of platinum for unitized regenerative fuel cell (URFC), Journal of Power Sources 195 (7) (2010) 1950–1956. `doi:10.1016/j.jpowsour.2009.10.002`.
URL `https://www.sciencedirect.com/science/article/pii/S0378775309017352`

[127] R. Petrone, D. Hissel, M. Péra, D. Chamagne, R. Gouriveau, Accelerated stress test procedures for PEM fuel cells under actual load constraints: State-of-art and proposals, International Journal of Hydrogen Energy 40 (36) (2015) 12489–12505. `doi:10.1016/j.ijhydene.2015.07.026`.
URL `https://linkinghub.elsevier.com/retrieve/pii/S0360319915017590`

[128] M. Carmo, D. L. Fritz, J. Mergel, D. Stolten, A comprehensive review on PEM water electrolysis, International Journal of Hydrogen Energy 38 (12) (2013) 4901–4934. `doi:10.1016/j.ijhydene.2013.01.151`.
URL `https://linkinghub.elsevier.com/retrieve/pii/S0360319913002607`

[129] EuropeanComission, Definition of Accelerated Stress Testing (AST) protocols deduced from understanding of degradation mechanisms of aged stack components in Fuel Cell systems | Programme | H2020, Tech. rep., European Comission.
URL `https://cordis.europa.eu/programme/id/H2020_FCH-04-5-2017`

[130] S. Escribano, F. Micoud, L. Guétaz, Development of exacerbated load cycles as AST for PEMFC stacks and validation by in-situ and ex-situ characterizations.

[131] K. Zhang, X. Liang, L. Wang, K. Sun, Y. Wang, Z. Xie, Q. Wu, X. Bai, M. S. Hamdy, H. Chen, X. Zou, Status and perspectives of key materials for PEM electrolyzer, Nano Research Energy 1 (2022) e9120032. `doi:10.26599/NRE.2022.9120032`.
URL `https://www.sciopen.com/article/10.26599/NRE.2022.9120032`

[132] C. Spöri, C. Brand, M. Kroschel, P. Strasser, Accelerated Degradation Protocols for Iridium-Based Oxygen Evolving Catalysts in Water Splitting Devices, Journal of The Electrochemical Society 168 (3) (2021) 034508. `doi:10.1149/1945-7111/abeb61`.
URL `https://iopscience.iop.org/article/10.1149/1945-7111/abeb61`

[133] C. Rozain, E. Mayousse, N. Guillet, P. Millet, Influence of iridium oxide loadings on the performance of PEM water electrolysis cells: Part II – Advanced oxygen electrodes, Applied Catalysis B: Environmental 182 (2016) 123–131. `doi:10.1016/j.apcatb.2015.09.011`.
URL `https://linkinghub.elsevier.com/retrieve/pii/S0926337315301417`

[134] S. Kundu, L. C. Simon, M. W. Fowler, Comparison of two accelerated Nafion™ degradation experiments, Polymer Degradation and Stability 93 (1) (2008) 214–224. `doi:10.1016/j.polymdegradstab.2007.10.001`.
URL `https://linkinghub.elsevier.com/retrieve/pii/S0141391007002960`

[135] J. H. Chun, D. H. Jo, S. G. Kim, S. H. Park, C. H. Lee, S. H. Kim, Improvement of the mechanical durability of micro porous layer in a proton exchange membrane fuel cell by elimination of surface cracks, Renewable Energy 48 (2012) 35–41. `doi:10.1016/j.renene.2012.04.011`.
URL `https://linkinghub.elsevier.com/retrieve/pii/S0960148112002522`

[136] C.-Y. Lee, C.-H. Chen, G.-B. Jung, S.-C. Li, Y.-Z. Zeng, Internal Microscopic Diagnosis of Accelerated Aging of Proton Exchange Membrane Water Electrolysis Cell Stack, Micromachines 11 (12) (2020) 1078. `doi:10.3390/mi11121078`.
URL `https://www.mdpi.com/2072-666X/11/12/1078`

[137] J. Wu, J. J. Martin, F. P. Orfino, H. Wang, C. Legzdins, X.-Z. Yuan, C. Sun, In situ accelerated degradation of gas diffusion layer in proton exchange membrane fuel cellPart I: Effect of elevated temperature and flow rate, Journal of Power Sources 195 (7) (2010) 1888–1894. `doi:10.1016/j.jpowsour.2009.10.022`.
URL `https://linkinghub.elsevier.com/retrieve/pii/S0378775309018242`

[138] A. A. Franco, M. Gerard, Multiscale Model of Carbon Corrosion in a PEFC: Coupling with Electrocatalysis and Impact on Performance Degradation, Journal of The Electrochemical Society 155 (4) (2008) B367. `doi:10.1149/1.2838165`.
URL `https://iopscience.iop.org/article/10.1149/1.2838165`

[139] K. H. Wong, E. Kjeang, Macroscopic In-Situ Modeling of Chemical Membrane Degradation in Polymer Electrolyte Fuel Cells, Journal of The Electrochemical Society 161 (9) (2014) F823–F832. `doi:10.1149/2.0031409jes`.
URL `https://iopscience.iop.org/article/10.1149/2.0031409jes`

[140] P. Aßmann, A. S. Gago, P. Gazdzicki, K. A. Friedrich, M. Wark, Toward developing accelerated stress tests for proton exchange membrane electrolyzers, Current Opinion in Electrochemistry 21 (2020) 225–233. `doi:10.1016/j.coelec.2020.02.024`.
URL `https://linkinghub.elsevier.com/retrieve/pii/S2451910320300557`

[141] N. Li, S. S. Araya, S. K. Kær, Investigating low and high load cycling tests as accelerated stress tests for proton exchange membrane water electrolysis, Electrochimica Acta 370 (2021) 137748. `doi:10.1016/j.electacta.2021.137748`.
URL `https://linkinghub.elsevier.com/retrieve/pii/S0013468621000372`

[142] X. Lu, B. Du, S. Zhou, W. Zhu, Y. Li, Y. Yang, C. Xie, B. Zhao, L. Zhang, J. Song, Z. Deng, Optimization of power allocation for wind-hydrogen system multi-stack PEM water electrolyzer considering degradation conditions, International Journal of Hydrogen Energy 48 (15) (2023) 5850–5872. `doi:10.1016/j.ijhydene.2022.11.092`. URL `https://linkinghub.elsevier.com/retrieve/pii/S0360319922053289`

[143] F. Parache, H. Schneider, C. Turpin, N. Richet, O. Debellemanière, Bru, A. T. Thieu, C. Bertail, C. Marot, Impact of Power Converter Current Ripple on the Degradation of PEM Electrolyzer Performances, Membranes 12 (2) (2022) 109. `doi:10.3390/membranes12020109`. URL `https://www.mdpi.com/2077-0375/12/2/109`

[144] A. Voronova, H. Kim, J. H. Jang, H. Park, B. Seo, Effect of low voltage limit on degradation mechanism during high-frequency dynamic load in proton exchange membrane water electrolysis, International Journal of Energy Research 46 (9) (2022) 11867–11878. `doi:10.1002/er.7953`. URL `https://onlinelibrary.wiley.com/doi/10.1002/er.7953`

[145] N. Zeng, C. Hu, C. Lv, A. Liu, L. Hu, Y. An, P. Li, M. Chen, X. Zhang, M. Wen, K. Chen, Y. Yao, J. Cai, T. Tang, Large-current density and high-durability proton exchange membrane water electrolysis for practical hydrogen isotope separation, Separation and Purification Technology 310 (2023) 123148. `doi:10.1016/j.seppur.2023.123148`. URL `https://linkinghub.elsevier.com/retrieve/pii/S1383586623000564`

[146] S. A. Grigoriev, D. G. Bessarabov, V. N. Fateev, Degradation mechanisms of MEA characteristics during water electrolysis in solid polymer electrolyte cells, Russian Journal of Electrochemistry 53 (3) (2017) 318–323. `doi:10.1134/S1023193517030065`. URL `https://doi.org/10.1134/S1023193517030065`

[147] Z. Ural, M. T. Gencoglu, Design and simulation of a solar-hydrogen system for different situations, International Journal of Hydrogen Energy 39 (16) (2014) 8833–8840. `doi:10.1016/j.ijhydene.2013.12.025`. URL `https://linkinghub.elsevier.com/retrieve/pii/S0360319913029583`

[148] M. Chandesris, V. Médeau, N. Guillet, S. Chelghoum, D. Thoby, F. Fouda-Onana, Membrane degradation in PEM water electrolyzer: Numerical modeling and experimental evidence of the influence of temperature and current density, International Journal of Hydrogen Energy 40 (3) (2015) 1353–1366. `doi:10.1016/j.ijhydene.2014.11.111`.
URL `https://linkinghub.elsevier.com/retrieve/pii/S0360319914032455`

[149] C. Briant, Z. Wang, N. Chollocoop, Hydrogen embrittlement of commercial purity titanium, Corrosion Science 44 (8) (2002) 1875–1888. `doi:10.1016/S0010-938X(01)00159-7`.
URL `https://linkinghub.elsevier.com/retrieve/pii/S0010938X01001597`

[150] H. Rezk, T. Wilberforce, E. T. Sayed, A. N. Alahmadi, A. Olabi, Finding best operational conditions of PEM fuel cell using adaptive neuro-fuzzy inference system and metaheuristics, Energy Reports 8 (2022) 6181–6190. `doi:10.1016/j.egyr.2022.04.061`.
URL `https://linkinghub.elsevier.com/retrieve/pii/S2352484722008265`